iScience

CellPress

Article

Loss of Adipose Growth Hormone Receptor in Mice Enhances Local Fatty Acid Trapping and Impairs Brown Adipose Tissue Thermogenesis

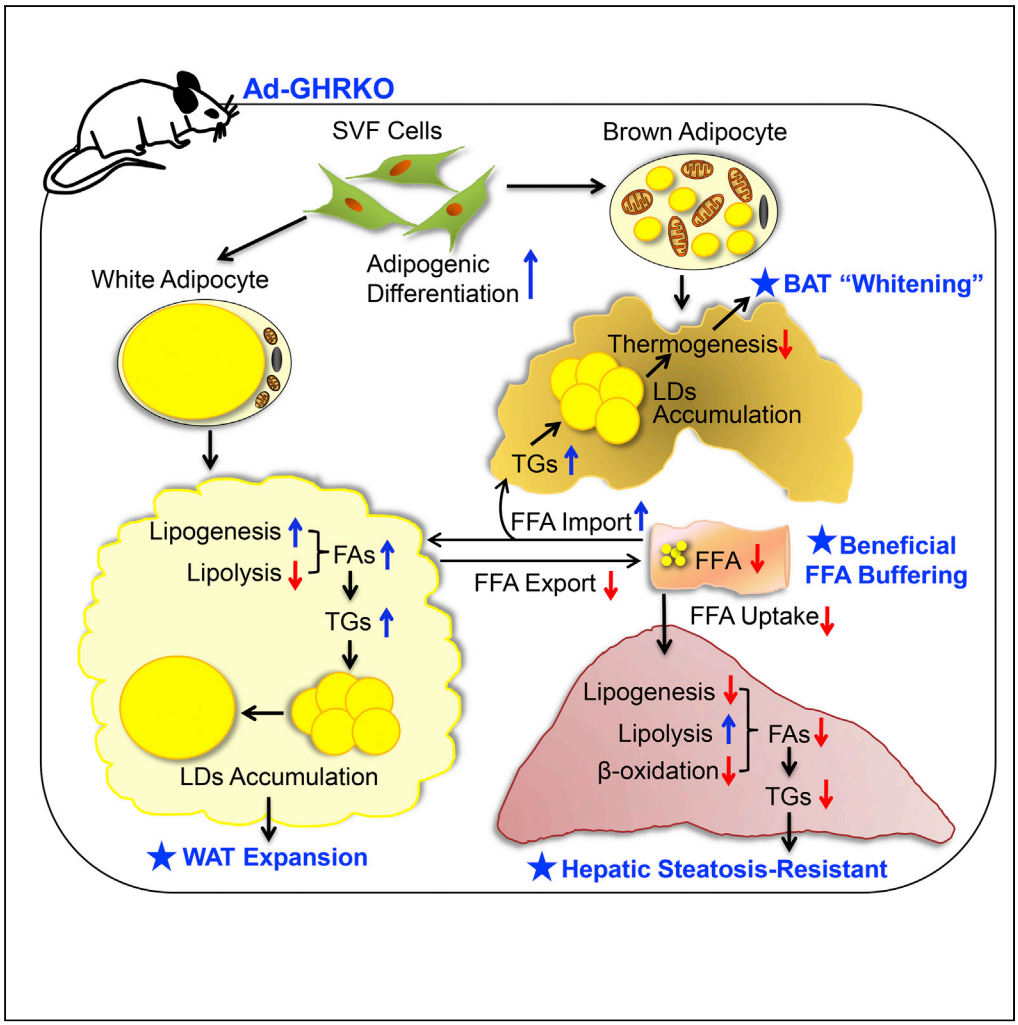

Liyuan Ran, Xiaoshuang Wang, Ai Mi, ..., Bin Liang, Xin Li, Yingjie Wu

liangb@mail.kiz.ac.cn (B.L.)
xl15@nyu.edu (X.L.)
yingjiewu@dmu.edu.cn (Y.W.)

HIGHLIGHTS

Adipose growth hormone receptor defect augments dietary obesity in mice

Lack of adipose growth hormone receptor prevents ectopic adiposity

Adipose growth hormone receptor defect benefits free fatty acid turnover

Adipose growth hormone receptor facilitates thermogenic response to cold

Ran et al., iScience *16*, 106–121
June 28, 2019
https://doi.org/10.1016/j.isci.2019.05.020

iScience

CellPress

Article

Loss of Adipose Growth Hormone Receptor in Mice Enhances Local Fatty Acid Trapping and Impairs Brown Adipose Tissue Thermogenesis

Liyuan Ran,[1,2,3,12] Xiaoshuang Wang,[1,2,3,12] Ai Mi,[1,2,3] Yanshuang Liu,[1,2] Jin Wu,[1,2,3] Haoan Wang,[1,2,3] Meihua Guo,[1,2,3] Jie Sun,[1,2,3,4] Bo Liu,[1,2,3] Youwei Li,[1,2,3] Dan Wang,[1,2,3] Rujiao Jiang,[1,2,3] Ning Wang,[1,2,3] Wenting Gao,[1,2,3] Li Zeng,[1,2] Lin Huang,[5] Xiaoli Chen,[6] Derek LeRoith,[7] Bin Liang,[8,*] Xin Li,[9,10,11,*] and Yingjie Wu[1,2,3,4,7,9,13,*]

SUMMARY

Growth hormone (GH) binds to its receptor (growth hormone receptor [GHR]) to exert its pleiotropic effects on growth and metabolism. Disrupted GH/GHR actions not only fail growth but also are involved in many metabolic disorders, as shown in murine models with global or tissue-specific *Ghr* deficiency and clinical observations. Here we constructed an adipose-specific *Ghr* knockout mouse model Ad-GHRKO and studied the metabolic adaptability of the mice when stressed by high-fat diet (HFD) or cold. We found that disruption of adipose *Ghr* accelerated dietary obesity but protected the liver from ectopic adiposity through free fatty acid trapping. The heat-producing brown adipose tissue burning and white adipose tissue browning induced by cold were slowed in the absence of adipose *Ghr* but were recovered after prolonged cold acclimation. We conclude that at the expense of excessive subcutaneous fat accumulation and lower emergent cold tolerance, down-tuning adipose GHR signaling emulates a healthy obesity situation which has metabolic advantages against HFD.

INTRODUCTION

Growth hormone (GH), secreted from the anterior pituitary, has profound effects on the regulation of growth and development throughout the life of mammals (Moller and Jorgensen, 2009; Baumann, 2009). The biological response of GH is primarily dependent on ligand binding to its membrane receptor, GHR (Flores-Morales et al., 2006). *Ghr* is predominantly expressed in the liver, and is also abundant in the fat and muscle. Laron syndrome (LS) is a specific hereditary disease caused by mutations in the *Ghr* gene that leads to GH insensitivity, despite sufficient GH secretion. Patients with LS exhibit short stature, delayed puberty, and truncal obesity (Laron et al., 1966; Rosenbloom, 1999). On the other hand, individuals with LS have very low cancer risk and rarely develop diabetes, implying that *Ghr* is intimately involved in glucose and lipid metabolism (Guevara-Aguirre and Rosenbloom, 2015; Laron, 2015; Janecka et al., 2016). These phenotypes of LS are well reproduced in the *Ghr* gene-disrupted mouse model ($GHR^{-/-}$) (Zhou et al., 1997; List et al., 2011). Going from LS to the other extreme, disturbance of glucose metabolism is one of the most common complications in patients with acromegaly with pituitary overproduction of GH. The prevalence and severity of diabetes in patients with acromegaly are considerably higher than those in other populations including people with high risk of diabetes (Dreval et al., 2014). Children with height at the upper end of gender- and age-specific scales were found to have greater adult adiposity and a higher risk of obesity onset than their shorter counterparts (Freedman et al., 2002; Stovitz et al., 2010). The unexpected uncoupling of obesity and type 2 diabetes observed in LS patients and related animal models prompts researchers to tease apart the exact role of adipose GHR in the multifaceted metabolic control.

The $GHR^{-/-}$ mice exhibit dwarfism, severe postnatal growth retardation, obesity, greatly decreased levels of serum insulin-like growth factor 1 (IGF-1), but elevated levels of GH, and longevity (List et al., 2011; Zhou et al., 1997; Berryman et al., 2006). Meanwhile, $GHR^{-/-}$ mice display enhanced insulin sensitivity and improved glucose homeostasis, even when challenged with high-fat (HF) diet (Coschigano et al., 2000, 2003; Dominici et al., 2000). Apart from the global *Ghr*-null models, tissue- and cell-specific *Ghr* knockout in liver (Fan et al., 2009; List et al., 2014), muscle (Vijayakumar et al., 2012a, 2012b; Mavalli et al., 2010; List et al., 2015), adipose tissues (List et al., 2013, 2019), macrophage (Lu et al., 2013), cardiac (Jara et al., 2016),

[1]Institute for Genome Engineered Animal Models of Human Diseases, Dalian Medical University, Dalian 116044, China

[2]National Center of Genetically Engineered Animal Models for International Research, Dalian Medical University, Dalian 116044, China

[3]Liaoning Provence Key Lab of Genome Engineered Animal Models, Dalian Medical University, Dalian 116044, China

[4]College of Integrative Medicine, Dalian Medical University, Dalian 116044, China

[5]Department of Pathophysiology, Dalian Medical University, Dalian 116044, China

[6]Department of Food Science and Nutrition, University of Minnesota, Twin Cities, MN, USA

[7]Division of Endocrinology, Diabetes and Bone Disease, Department of Medicine, Icahn Mount Sinai School of Medicine, New York 10029, USA

[8]Key Laboratory of Animal Models and Human Disease Mechanisms of the Chinese Academy of Sciences & Yunnan Province, Kunming Institute of Zoology, Center for Excellence in Animal Evolution and Genetics, Chinese Academy of Sciences, Kunming 650223, China

[9]Department of Basic Science and Craniofacial Biology, New York University College of Dentistry, New York 10010, USA

Continued

and islet β cell (Wu et al., 2011) have been generated in mice, which have provided detailed information on physiological functions of GH signaling in local tissues. Most of the tissue-specific *Ghr* knockout (KO) mice showed similarities to $GHR^{-/-}$ mice (Wu et al., 2011; Vijayakumar et al., 2012a, 2012b; List et al., 2013, 2014; Fan et al., 2009; Sun and Bartke, 2014).

The adipose organ is composed of white and brown/beige adipocytes that are respective major sites of energy storage and cold-adapted thermogenesis. White adipose tissue (WAT) is predominately used to store excess energy in the form of triglycerides (TGs) and to provide free fatty acids (FFAs) under conditions of starvation or energy deficiency. In addition, WAT releases several important adipokines to regulate metabolic homeostasis. Cold exposure or β-adrenergic stimulation could induce browning of WAT, which results in a distinct type of fat cells called "beige adipocytes." The increase of beige adipose has anti-obesity and anti-diabetic benefits (Giralt and Villarroya, 2013; Schrauwen et al., 2015). As a thermogenic organ in mammals, brown adipose tissue (BAT) is characterized by a high mitochondrial content to maintain normal body temperature and is involved in energy expenditure (Nicholls and Locke, 1984). The mitochondria within BAT are rich in uncoupling protein 1 (UCP1), which can dissipate chemical energy as heat through uncoupling oxidative respiration and ATP synthesis (Cohen and Spiegelman, 2015). Excess expansion of WAT, deficiency of thermogenic capacity, and low expression of *Ucp1* gene in BAT have been linked to obesity and various metabolic diseases (Chathoth et al., 2018; Rui, 2017; Bonet et al., 2017; Bond and Ntambi, 2018).

The first adipose-specific deletion of *Ghr* mouse model (FaGHRKO) was reported by List et al., using adipocyte protein 2 (aP2) promoter as the Cre recombinase driver (List et al., 2013). Both $GHR^{-/-}$ and FaGHRKO mice displayed enlarged fat mass and adipocyte size (Zhou et al., 1997; List et al., 2013). The unexpected mild phenotypes of FaGHRKO, such as altered fat composition, lower circulating IGF-1, and leptin levels (List et al., 2013), were soon explained by the leaked activity of the aP2 promoter in many non-adipose cells types including macrophages and skeletal muscle (Wang et al., 2010; Lee et al., 2013). Utilization of different Cre mouse deletion strains and variance in diet schemes further confused the phenotype interpretation. Apart from the $GHR^{-/-}$ and FaGHRKO model, an adiponectin-Cre-driving adipocyte-specific GHRKO mice (AdGHRKO) was generated by List et al. during preparation of this study (List et al., 2019). The phenotypes of several other tissue-specific GHRKO mouse lines were exacerbated by HF diet (Lu et al., 2013, Wu et al., 2011), but both FaGHRKO and AdGHRKO did not try HF treatment. In the present work, we constructed an adiponectin-driven Cre transgenic mouse line (Ad-GHRKO) to attain targeted *Ghr* deletion in adipose. The high specificity and efficacy of the model provided an ideal tool to discern the contribution of adipose GH/GHR to the fat-related metabolic aberrance.

Excessive calorie intake from opulent eating has been fueling the epidemic of metabolic disorders. Therefore the leverage of adipose *Ghr* on susceptibility to dietary obesity and liver lesions was analyzed in this study with particular interest. Recently, GH's anti-obesity action has also been reported to be correlated with "browning" of inguinal white adipose (Nelson et al., 2018). Less effective adaptive thermogenesis is claimed to be the major cause of failure or the high recidivism rate of weight loss therapy (Dulloo and Schutz, 2015), in which GH interacts with neuroendocrine hormones and other metabolic and psychobehavioral factors to actively defend body energy storage. BAT thermogenesis in global GHRKO and Ames dwarf mice, the latter being depleted of GH/IGF-1 signaling and thyroid hormone function, were significantly enhanced (Darcy et al., 2016; Darcy and Bartke, 2017; Archana et al., 2011). However, the roles of GH in adipose thermogenesis had heavily interfered with systemic changes unrelated to GH action or alterations in multiple hormonal axes in these models. The functional roles of adipose *Ghr* control of adaptive thermogenesis remain unknown, which is the main focus of this study.

RESULTS

Generation and Characterization of Ad-GHRKO Mice

Beyond aP2 promoter, adiponectin (Adipoq) promoter serves as a second-generation adipose-targeting driver for gene engineering. We created an adipose-specific *Ghr* gene knockout (Ad-GHRKO) mouse model by crossing GHR-Floxed (Flox) mice with Adipoq-Cre mice (Figures 1A and 1B). The efficiency and specificity of *Ghr* deletion in the fat pads were validated at DNA and mRNA levels (Figures 1C and 1D). PCR genotyping with the primers listed in Table S1 showed that the Cre activity driven by the Adipoq promoter mediated adipocyte-specific *Ghr* disruption without affecting other tissues (Figure 1C). The mRNA expression level of *Ghr* was significantly and sufficiently decreased in most adipose tissues (Figure 1D).

[10]Department of Urology, New York University Langone Medical Center, New York 10016, USA

[11]Perlmutter Cancer Institute, New York University Langone Medical Center, New York 10016, USA

[12]These authors contributed equally

[13]Lead Contact

*Correspondence: liangb@mail.kiz.ac.cn (B.L.), xl15@nyu.edu (X.L.), yingjiewu@dmu.edu.cn (Y.W.)

https://doi.org/10.1016/j.isci.2019.05.020

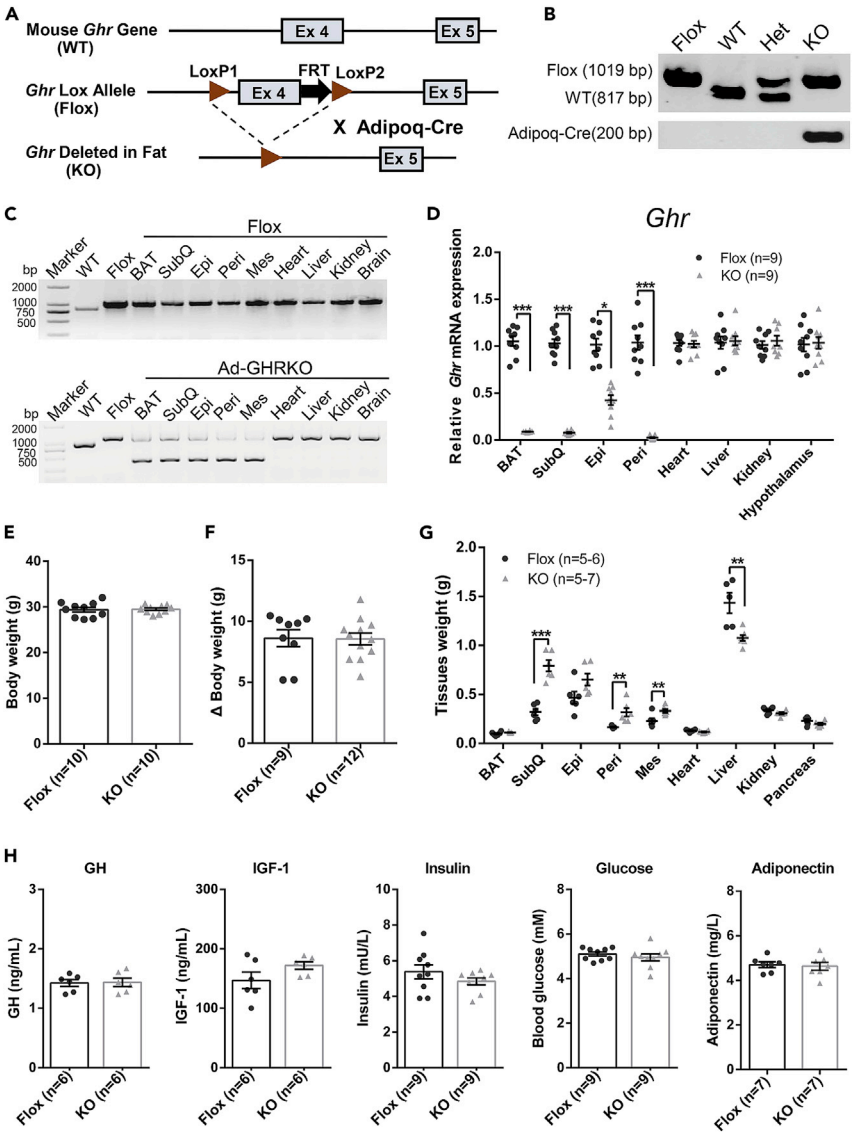

Figure 1. Generation and Characterization of Adipose-Specific *Ghr* Knockout Mice

(A) Schematic diagram of Ad-GHRKO mice construction.

(B) PCR genotyping of Flox and KO mice.

(C and D) PCR (C) and real-time PCR (D) analyses of *Ghr* expression level in various tissues. Note that a smaller deletion band due to Cre excision was detected only in adipose tissues of KO mice.

(E and F) The body weight (E) and increase in body weight (20 weeks versus 4 weeks) (F) of male Ad-GHRKO and Flox mice 20 weeks old.

(G) Tissues weight of male Ad-GHRKO and Flox mice 20 weeks old.

(H) Serum GH, IGF-1, insulin, blood glucose, and adiponectin levels of 20-week-old male Flox and Ad-GHRKO mice. WT, wild type; Flox, GHR-Floxed; KO, Ad-GHRKO; Het, heterozygote; BAT, brown adipose tissue; SubQ, subcutaneous white adipose tissue; Epi, epididymal white adipose tissue; Peri, perigonadal white adipose tissue; Mes, mesenteric white adipose tissue.

All values are presented as mean ± SEM. Statistical significance is shown as *$p \leq 0.05$, **$p \leq 0.01$, and ***$p \leq 0.001$. See also Table S2.

To determine the effect of *Ghr* deficiency on body weight and composition, the body and organ weight of 20-week-old mice were measured. Unlike the FaGHRKO mice (List et al., 2013), no obvious differences in body weight and increase of body weight were observed between Ad-GHRKO and control mice in the rearing period (Figures 1E and 1F). Except for the BAT, all the different fat depots examined in Ad-GHRKO mice

were heavier than the control (Figure 1G). Among them, the subcutaneous (subQ) WAT had the largest increase of weight, whereas the liver was markedly lighter and the weights of other tissues like the heart, kidney, and pancreas were slightly reduced in Ad-GHRKO mice (Figure 1G). We calculated the sum of the weight increase of the WAT fat pads and the weight decrease in the liver, heart, kidney, and pancreas. The results showed that the Ad-GHRKO mice had 0.996 ± 0.162 g weight gain in WAT, which was not equal to the 0.456 ± 0.194 g weight loss in other organs altogether. Among these organs, the liver was the only one displaying a significant decrease. Although other body parts such as muscles and bone were not measured, we concluded that the decreased liver weight was the principal, but not the only factor contributing to the unchanged body weight of Ad-GHRKO mice. Serological detection indicated that loss of *Ghr* in adipose tissues had little effect on circulating GH and IGF-1 levels in Ad-GHRKO mice (Figure 1H). Serum insulin, blood glucose levels, and adiponectin level also do not display any notable differences between 20-week-old Ad-GHRKO and Flox mice (Figure 1H).

The Absence of Adipose *Ghr* Exacerbated Diet-Induced Obesity but Improved Glucose Homeostasis

The weight gain of both Ad-GHRKO mice and the control littermates stayed in step with each other under regular chow, whereas an incrementally enlarged gap emanated between the two groups when fed with HF diet for 16 weeks (HF diet feeding was started from age 8 weeks) (Figures 2A–2C). Anatomical dissections revealed that the heavier body weight in Ad-GHRKO mice mainly originated from more weight gain in adipose tissues, especially the subcutaneous, perirenal, and mesenteric WAT (Figure 2D).

It has been reported that $GHR^{-/-}$ and AdGHRKO mice exhibited healthy adipose expansion with improved insulin sensitivity (Liu et al., 2004; Coschigano et al., 2003; Arum et al., 2014; List et al., 2019), whereas the basal glucose homeostasis of FaGHRKO mice was not changed (List et al., 2013). In good agreement with this, no significant difference was found in the serum glucose level in mice with or without adipose *Ghr* deletion, when fed with regular chow (RC). After loading with HF diet for 8 weeks, fasting blood glucose level in Ad-GHRKO mice was significantly lower than in Flox mice (KO 8.31 ± 1.18 mmol/L versus Flox 11.34 ± 0.44 mmol/L) (Figure 2E). Glucose tolerance test and insulin tolerance test assays revealed that Ad-GHRKO mice were more sensitive to insulin stimulation than control littermates after 8 weeks of HF diet (Figures 2G and 2H). With prolonged HF diet for 16 weeks, the fasted blood glucose level in Ad-GHRKO mice was still lower than that of the control mice (KO 8.63 ± 1.28 mmol/L versus Flox 10.26 ± 1.06 mmol/L) (Figure 2F), and Ad-GHRKO mice responded better to glucose challenge (Figure 2I) but no longer showed advantage in insulin sensitivity (Figure 2J). Overall, these results indicated that defective adipose GH signaling rescued, to a significant degree, the mice from hyperglycemia and insulin resistance imposed by oversupplied nutrients.

An Integration of Lipolysis, Lipogenesis, and Adipogenesis Magnified the HF-Induced Obesity and Limited FFA Liberation in Ad-GHRKO Mice

The obesity in $GHR^{-/-}$, FaGHRKO, and AdGHRKO mice was attributed to fat expansion in both number and size of adipocytes (Zhou et al., 1997; Arum et al., 2014; List et al., 2013, 2019). As we expected, the subQ WATs of Ad-GHRKO mice were significantly larger than those of the control littermates when fed with RC, which was exaggerated by HF diet treatment (Figures 3A–3C). Furthermore, we examined the expression levels of lipid metabolism-related genes (Primers are listed in Table S1) and proteins. As expected, lipolysis-related genes (e.g., *Atgl*, *Hsl*, *Mgl*) were down-regulated, whereas genes involved in lipogenesis (e.g., *Pparγ*, *Acc1*, *Fas*) were up-regulated (Figure 3D) in subQ WAT of KO mice. The expression of *Fsp27* gene, which encodes fat-specific protein 27 (Fsp27) and is an important positive regulator for fat droplet formation, was significantly higher in Ad-GHRKO mice than in the controls, especially when challenged with HF diet (Figure 3D). Consistently, the western blot results showed that deficiency of *Ghr* in adipose tissues dramatically enhanced the levels of ACC1, FAS, SREBP1, and PPARγ (Figure 3E). Although higher circulatory FFAs are commonly detected in obese individuals owing to expanded fat mass, serum FFA levels were comparable in the Ad-GHRKO versus control mice (Figure 3F). More intriguingly, despite the augmented obesity after HF diet, the FFA release of Ad-GHRKO mice was only mildly elevated by excessive feeding and was significantly lower than that of the HF-fed Flox control (Figure 3F). The data implied that lack of GHR in adipose improved local FFA recycling, which could provide a beneficial FFA buffering for systemic glucose metabolism and ectopic fat deposition in the liver.

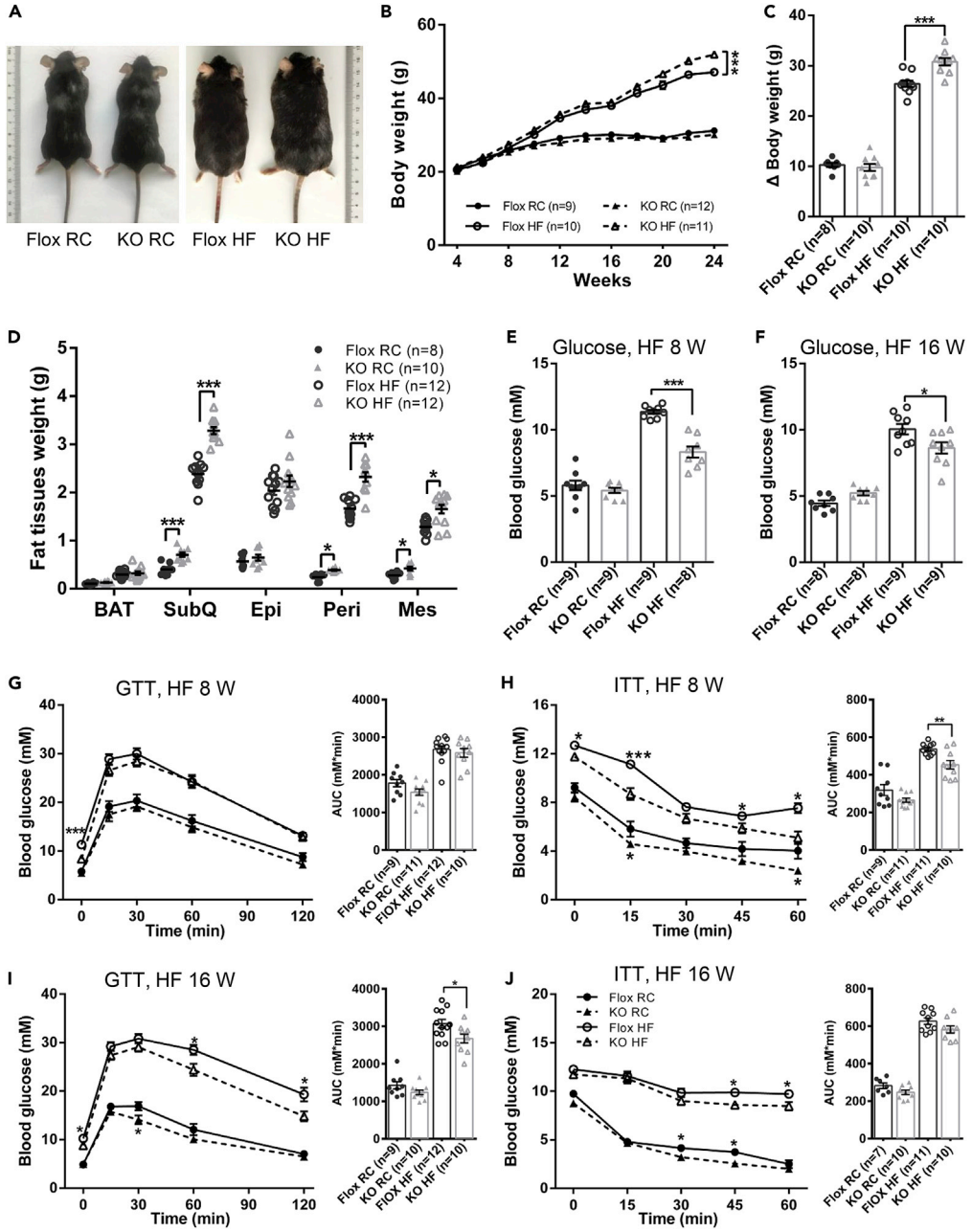

Figure 2. Ad-GHRKO Exacerbates Dietary Obesity but Improves Glucose Homeostasis during HF Feeding

(A) Representative photographs of 24-week-old male Ad-GHRKO and Flox mice (HF fed for 16 weeks).

(B)The growth curves of Ad-GHRKO and Flox mice during RC or HF feeding.

(C) Increase in body weight (24 weeks versus 4 weeks) of 24-week-old male Ad-GHRKO and Flox mice (HF fed for 16 weeks).

(D) Fat tissue weight of 24-week-old male Ad-GHRKO and Flox mice (HF fed for 16 weeks).

(E and F) Fasting blood glucose levels of Ad-GHRKO and Flox mice fed with HF for 8 (E) and 16 weeks (F).

(G–J) Glucose tolerance test and insulin tolerance test of Ad-GHRKO and Flox mice fed with HF for 8 (G and H) and 16 weeks (I and J). Inset: The area under curves.

All values are presented as mean ± SEM. Statistical significance is shown as *$p \leq 0.05$, **$p \leq 0.01$, and ***$p \leq 0.001$. See also Figures S1 and S5 and Table S2.

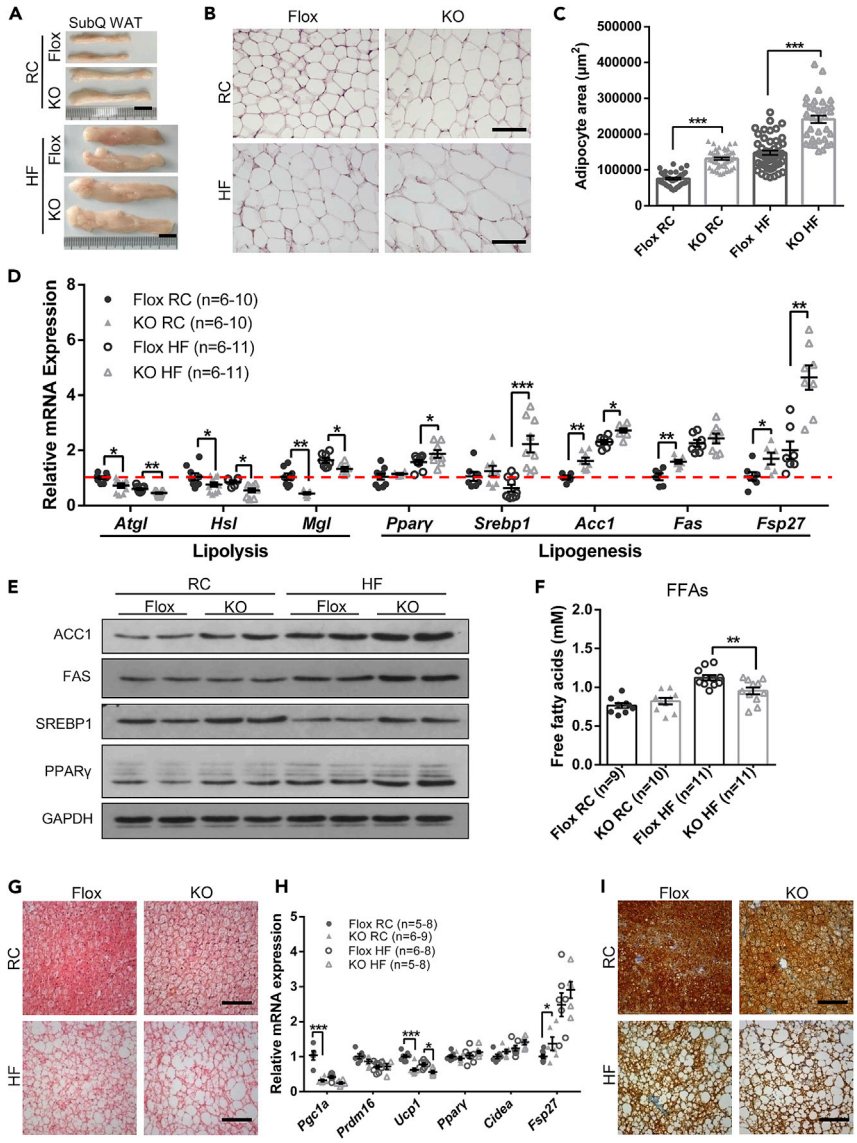

Figure 3. Ad-GHRKO Causes Lipid Accumulation in WAT and BAT

(A) Representative images of SubQ WAT from 24-week-old male Ad-GHRKO and Flox mice (HF fed for 16 weeks). Scale bar, 1 cm.

(B) H&E staining of SubQ WAT from 24-week-old male Ad-GHRKO and Flox mice (HF fed for 16 weeks). Scale bar, 100 μm.

(C) Quantification of adipocyte area of SubQ WAT.

(D) Relative expression levels of genes related to lipolysis and lipogenesis in SubQ WAT from 24-week-old male Ad-GHRKO and Flox mice (HF fed for 16 weeks).

(E) The levels of selected proteins in SubQ WAT of 24-week-old male Ad-GHRKO and Flox mice (HF fed for 16 weeks).

(F) Serum FFA levels of 24-week-old male Ad-GHRKO and Flox mice (HF fed for 16 weeks).

(G) BAT sections stained with H&E in 24-week-old male Ad-GHRKO and Flox mice (HF fed for 16 weeks). Scale bar, 100 μm.

(H) Relative expression levels of genes related to thermogenesis and lipogenesis in BAT of 24-week-old male Ad-GHRKO and Flox mice (HF fed for 16 weeks).

(I) Immunostaining of BAT sections with anti-UCP-1 antibody. Scale bar, 100 μm.

All values are presented as mean ± SEM. Statistical significance is shown as *$p \leq 0.05$, **$p \leq 0.01$, and ***$p \leq 0.001$. See also Table S2.

Histology analysis showed that lipid droplet expansion and accumulation were displayed in BAT of Ad-GHRKO mice (Figure 3G). Compared with the Flox mice, the Ad-GHRKO mice had greatly increased expression of genes involved in fatty acid synthesis and lipid droplet accumulation (e.g., *Ppar-γ*, *Cidea*, and *Fsp27*) in BAT (Figure 3H). Meanwhile, the expression levels of thermogenic genes such as *Pgc1α*, *Prdm16*, and *Ucp1* were significantly reduced in BAT by GHR deletion (Figure 3H). Consistent with the mRNA data, the staining of BAT UCP1 was significantly lower in Ad-GHRKO mice than in the controls, especially when challenged with HF diet (Figure 3I).

Not only adipocyte hypertrophy but also hyperplasia through activation of the adipogenic SVF cells contributes to obesity. SVF cells are a mixed cell population rich in pre-adipocytes, mesenchymal stem cells, and various inflammatory cells (Schipper et al., 2012; Riordan et al., 2009). The effect of *Ghr* disruption on adipocyte regeneration was determined by adipogenic differentiation of SVF cells separated from adipose tissues, *in vitro*. Consistent with *in vivo* experiments, the SVF cells isolated from WAT and BAT of KO mice showed higher differentiation potential (Figures 4A and 4B). Palmitic acid treatment, which simulated fatty acid influx, dose dependently increased the lipid droplets formation in the WAT SVF cells derived from Ad-GHRKO mice (Figure 4A). In addition, significant decreases in lipolysis gene (e.g., *Atgl*, *Hsl*) and increases in lipogenesis gene (e.g., *Acc*, *Fas*, *Fsp27*) expressions were observed in WAT SVF of Ad-GHTKO mice (Figure 4C). The results confirmed the participation of adipocyte differentiation in WAT expansion in adipose GHR-depleted mice. Meanwhile, SVF cells separated from BAT of Ad-GHRKO mice were more easily differentiated into adipocytes with lower expression levels of thermogenesis genes (e.g., *Ucp1*, *Pgc1a*) and lipolysis genes (e.g., *Atgl*, *Hsl*) and higher expression levels of lipogenesis genes (e.g., *Acc*, *Fas*, *Cidea*) than of the Flox mice (Figure 4D). Based on these results, we speculated that GHR could be required in the BAT thermogenic process, which is assessed in a later sector in the study.

Ad-GHRKO Mice Were More Resistant to HF-Induced Hepatic Steatosis

GH-stimulated hepatic secretion is the primary source of circulating IGF-1 (Sjogren et al., 1999). Serum levels of GH and IGF-1 have been shown to correlate with hepatic fat accumulation (Berryman et al., 2013). As a major site of lipogenesis and lipid oxidation, the liver is the central engine modulating whole-body metabolic homeostasis and is vulnerable to nutritional damage. We found that both the liver mass and liver index of Ad-GHRKO groups were significantly lower than those of the Flox mice, with or without HF diet stimuli (Figures 5A and 5B). Furthermore, deletion of *Ghr* in adipose brought down the liver TG contents significantly by 26.7% and 11.5% in mice fed with RC and HF for 16 weeks (Figure 5C), respectively. However, no apparent differences under RC condition were observed in hepatic histopathology by H&E and oil red O staining (Figure 5E). A significant increase of hepatic steatosis marked by vacuolated and lipid-laden hepatocytes was observed in both groups fed with HF for 16 weeks, but more manifest in the Flox mice than Ad-GHRKO mice (Figure 5E). The histopathologic changes and lipid deposit (Figure S1A, indicated by black arrows) occurred evidently in the liver of the Flox mice after only 8 weeks of HF feeding but not of the Ad-GHRKO mice (Figure S1A). Periodic acid-Schiff reaction of liver tissues showed that Ad-GHRKO mice have stronger glycogen synthesis capacity (Figure S1). The improvement of hepatic glycogen synthesis in Ad-GHRKO mice was conducive to the maintenance of blood glucose levels during HF feeding (Figures 2E and 2F). β-Hydroxybutyric acid (β-HBA) is the ketone body that indicates liver uptake of FFAs because it can only be produced from the mitochondrial β-oxidation of FFAs in the liver. Indeed, the serum β-HBA level in the HF-fed Ad-GHRKO mice was significantly lower than that in the Flox mice (Figure 5D). In conjunction with the lower FFA availability in Ad-GHRKO mice (Figure 3F), the results further demonstrated that an adipose FFA trapping is the mechanism underlying the hepatic protection against HF. The release of a variety of hepatic inflammation markers such as aspartate aminotransferase (AST) and alanine aminotransferase (ALT) is a biochemical sign indicating the loss of hepatocellular integrity. Compared with control littermates, a significant reduction in relative activity of both AST and ALT was observed in Ad-GHRKO mice fed with HF (Figure 5F). The influence of adipose *Ghr* deficiency on lipid profile was examined by measuring the serum triglyceride (TG), total cholesterol (T-CHO), high-density lipoprotein cholesterol (HDL-C), and low-density lipoprotein cholesterol (LDL-C) values. Despite the comparable baseline concentrations, the serum TG, T-CHO, and LDL-C in Ad-GHRKO groups were still significantly lower than in Flox mice under HF diet condition (Figures 5G–5J), confirming a suppressed development of hyperlipidemia in Ad-GHRKO mice.

In light of the findings of less lipid accumulation in the liver and a shrinking lipid and FFA reservoir in the circulation of Ad-GHRKO mice, we investigated whether the hepatic lipid turnover was directly altered. Compared with Flox mice under the same diet condition, the expression levels of lipogenic genes in

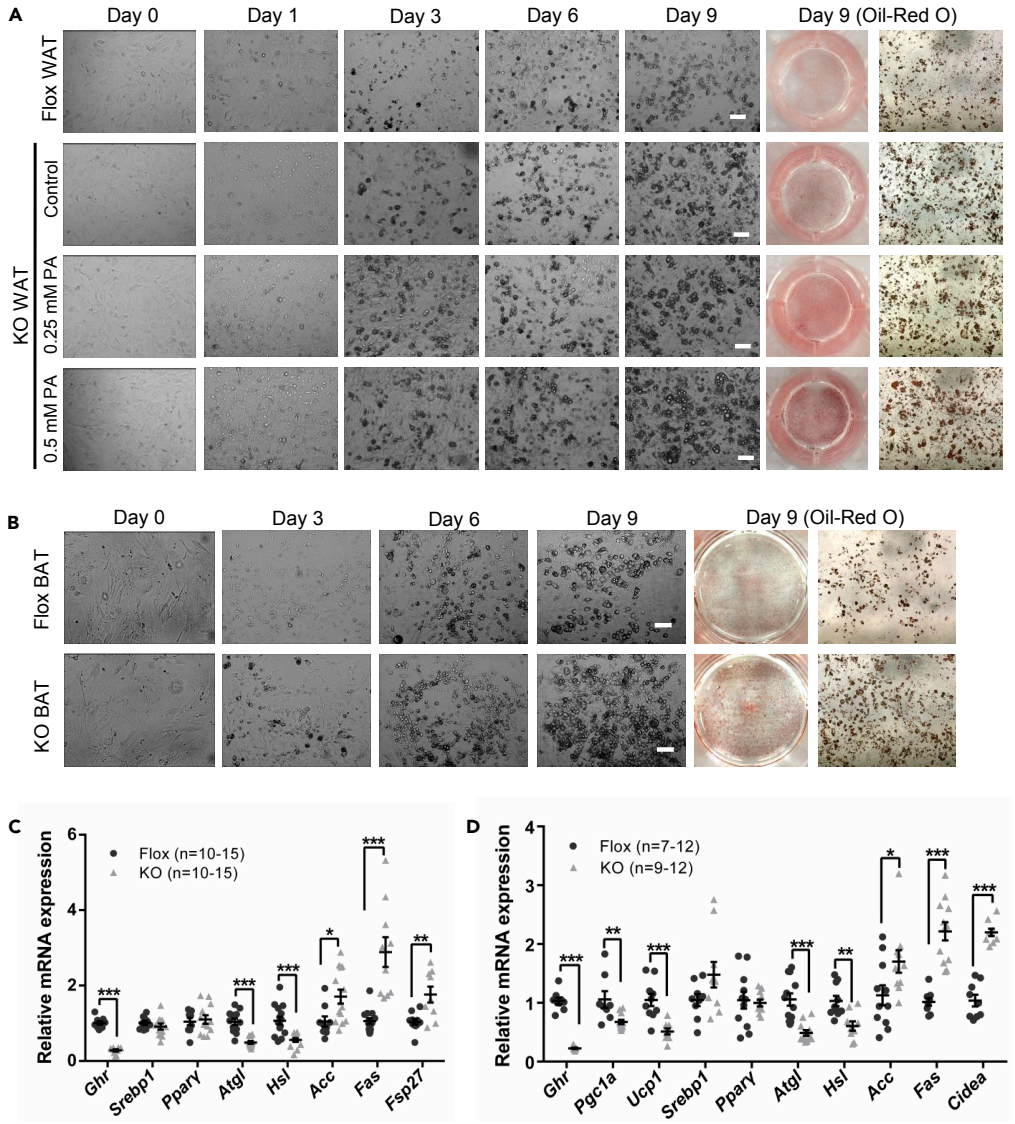

Figure 4. Deletion of *Ghr* in Adipocytes Promotes Adipogenic Differentiation of SVF Cells

(A) Induced adipogenic differentiation of SVF cells from subQ WAT of 20-week-old male Ad-GHRKO and Flox mice. Scale bar, 50 μm.

(B) Induced adipogenic differentiation of SVF cells from BAT of 20-week-old male Ad-GHRKO and Flox mice. Scale bar, 50 μm.

(C) Expression of *Ghr* and genes related to lipolysis and *de novo* lipogenesis in SVF cells from subQ WAT of 20-week-old male Ad-GHRKO and Flox mice.

(D) Expression of *Ghr* and genes related to thermogenesis, lipolysis, and *de novo* lipogenesis in SVF cells from BAT of 20-week-old male Ad-GHRKO and Flox mice.

All values are presented as mean ± SEM. Statistical significance is shown as *$p \leq 0.05$, **$p \leq 0.01$ and ***$p \leq 0.001$.

the liver of Ad-GHRKO were slightly lower or even had no significant changes (e.g., *Acc-1*, *Fas*), whereas the expression of genes involved in lipolysis (e.g., *Atgl*, *Hsl*, *Mgl*) were markedly increased with statistical significance (Figure 5K). There were no significant differences in the expression of *Pparα*, *Cpt2*, and *Atp5a*. Down-regulation of *Cpt1b* and *Fabp3* was detected in KO mice fed HF or RC diet (Figure 5K). We further found that the expression levels of genes related to fatty acid uptake, such as *Cd36* and *Fbtp2*, were significantly lower in Ad-GHRKO than in Flox mice under HF diet condition (Figure 5K). In contrast to the Ad-GHRKO mice, the protein abundances of FAS and CD36 displayed a striking increase in Flox mice when fed with HF diet (Figure 5L). Meanwhile, the levels of PPARα and ATGL, responsible for

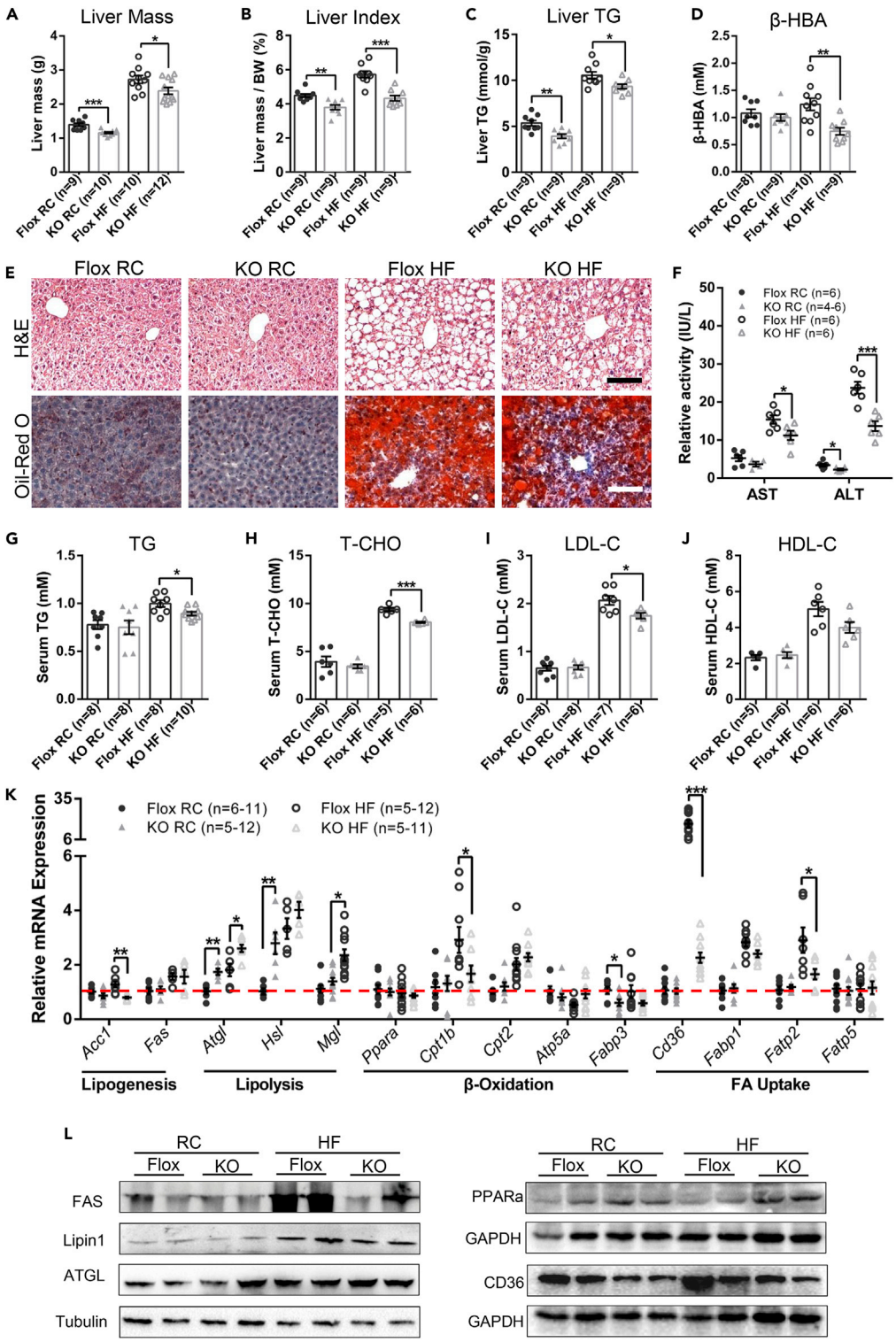

Figure 5. Ad-GHRKO Alleviates Hepatic Steatosis during HF Feeding

(A–C) Liver mass (A), liver index (liver weight/body weight %) (B), and liver triglyceride content (C) of 24-week-old male Ad-GHRKO and Flox mice (HF fed for 16 weeks).

(D) Serum β-HBA levels of 24-week-old male Ad-GHRKO and Flox mice (HF fed for 16 weeks).

(E) H&E and oil red O staining of liver sections of 24-week-old male Ad-GHRKO and Flox mice (HF fed for 16 weeks). Scale bar, 100 μm.

Figure 5. *Continued*

(F) Serum AST and ALT activity of 24-week-old male Ad-GHRKO and Flox mice (HF fed for 16 weeks).

(G–J) Serum TG (G), T-CHO (H), LDL-C (I), and HDL-C (J) levels of 24-week-old male Ad-GHRKO and Flox mice (HF fed for 16 weeks).

(K) Relative gene expression levels in livers of 24-week-old male Ad-GHRKO and Flox mice (HF fed for 16 weeks).

(L) Western blot analysis of proteins involved in *de novo* lipogenesis, lipolysis, β-oxidation, and FFA uptake in livers of 24-week-old male Ad-GHRKO and Flox mice (HF fed for 16 weeks).

All values are presented as mean ± SEM. Statistical significance is shown as *$p \leq 0.05$, **$p \leq 0.01$, and ***$p \leq 0.001$. See also Figure S1 and Table S2.

fatty acid disposal and lipolysis, respectively, were up-regulated in Ad-GHRKO mice, especially when challenged with HF diet (Figure 5L). Phospholipids are the main components of lipid and are involved in adipogenesis. Lipin1 is known as a phosphatidic acid phosphohydrolase enzyme that catalyzes the conversion of phosphatidate to diacylglycerol in the cytoplasm (Han et al., 2006; Qi et al., 2017). Lipin1 is also expressed as a nuclear transcriptional coactivator to modulate the expression of other genes involved in lipid metabolism (Peterson et al., 2011). Up-regulation of Lipin 1 is implicated in hepatic steatosis. As we expected, the basal and HF-stimulated Lipin1 expression were higher in Flox mice than in Ad-GHRKO mice (Figure 5L). These results coalesced to demonstrate that the adipose-tissue-specific ablation of *Ghr* protected the liver from diet-induced steatosis via the sum of promoted lipolysis and dampened lipogenesis at both transcriptional and translational levels. Most importantly, the absence of adipose *Ghr* pathway trapped fatty acid locally in WAT and thereby restrained the fatty acid delivery necessary for lipid production in the liver.

Adipose *Ghr* Signaling Was Required in the Cold-Stimulated Adaptive Thermogenesis

The high expression level of UCP1 is closely related to reduced body weight and increased insulin sensitivity (Kozak and Anunciado-Koza, 2008; Bond and Ntambi, 2018). PGC1α is a transcription co-activator related to mitochondrial function and adaptive thermogenesis (Puigserver et al., 1998). As we had observed above, BAT of Ad-GHRKO mice showed a "whitening" trend (Figure 3G). Besides, a down-regulation of thermogenic genes such as *Pgc1α*, *Prdm16,* and *Ucp1* was detected in BAT tissue (Figure 3H) and BAT-originated SVF cells (Figure 4D) of Ad-GHRKO mice. Consistent with mRNA data, protein levels of UCP1 were significantly reduced in BAT of Ad-GHRKO mice, especially in HF-feeding condition (Figure 3I). H&E staining showed that cold exposure reduced the lipid accumulation in BAT of Ad-GHRKO mice, but qPCR and immunohostochemistry analysis demonstrated that the expression levels of UCP1 and PGC1α were still lower in BAT of KO mice than in Flox mice (Figures 6A and S2A). As UCP1 is the key mediator in adaptive thermogenesis, its down-regulation in Ad-GHRKO mice implied the potential involvement of GHR in energy expenditure and emergent heat generation.

To test the hypothesis, the mice were stressed under 4°C on a 10-/14-h cycle for 9 days and body temperature changes were recorded. On the first day of the experiment, the rectal temperature of RC-fed Ad-GHRKO mice dropped more sharply than that of the Flox mice during the cold exposure (KO 26.15 ± 2.34°C versus Flox 31.06 ± 2.86°C at the end of 10-h exposure) (Figure 6B). Consistently, the rectal temperatures of KO mice also recovered more slowly in room temperature after cold acclimation (Figure 6C). However, in the mouse groups fed with HF diet for 8 weeks, adipose *Ghr* knockout had no impact on the decrease and recovery rates of the rectal temperature (Figures 6B and 6C, dashed lines). The cold endurance of all four groups of mice, with deficient or intact adipose *Ghr* and regardless of the diet, had no significant difference in the fluctuations of body temperature from the second to the ninth day of cold induction (Figures S3 and S4). In addition, the Flox control lost more weight following cold stimulation than the Ad-GHRKO mice, under both HF and RC feeding conditions (Figure 6D). When subQ WAT mass was examined, the cold acclimation only caused statistically significant weight reduction in the Flox mice, not the Ad-GHRKO mice (Figure 6E). The browning capacity of WAT of Ad-GHRKO mice in response to cold stimulation for 9 days was also impaired as shown by the remarkable darkening of the subQ fat tissues of the Flox mice, but not the Ad-GHRKO mice (Figure 6F). Histological examination revealed that the cold-Flox-RC group had a new population of "beige" fat cells, which contain multiple small lipid droplets and high levels of UCP1 and PGC1α, which was not detected in the cold-KO-RC group (Figure 6G). Consistently, the expression of marker genes of beige and thermogenesis in subQ WAT (Figure S2B) and epi WAT (Figure S2C) were declined in Ad-GHRKO mice. These results confirmed the requirement of adipose GHR for emergent heat production and cold adaptation.

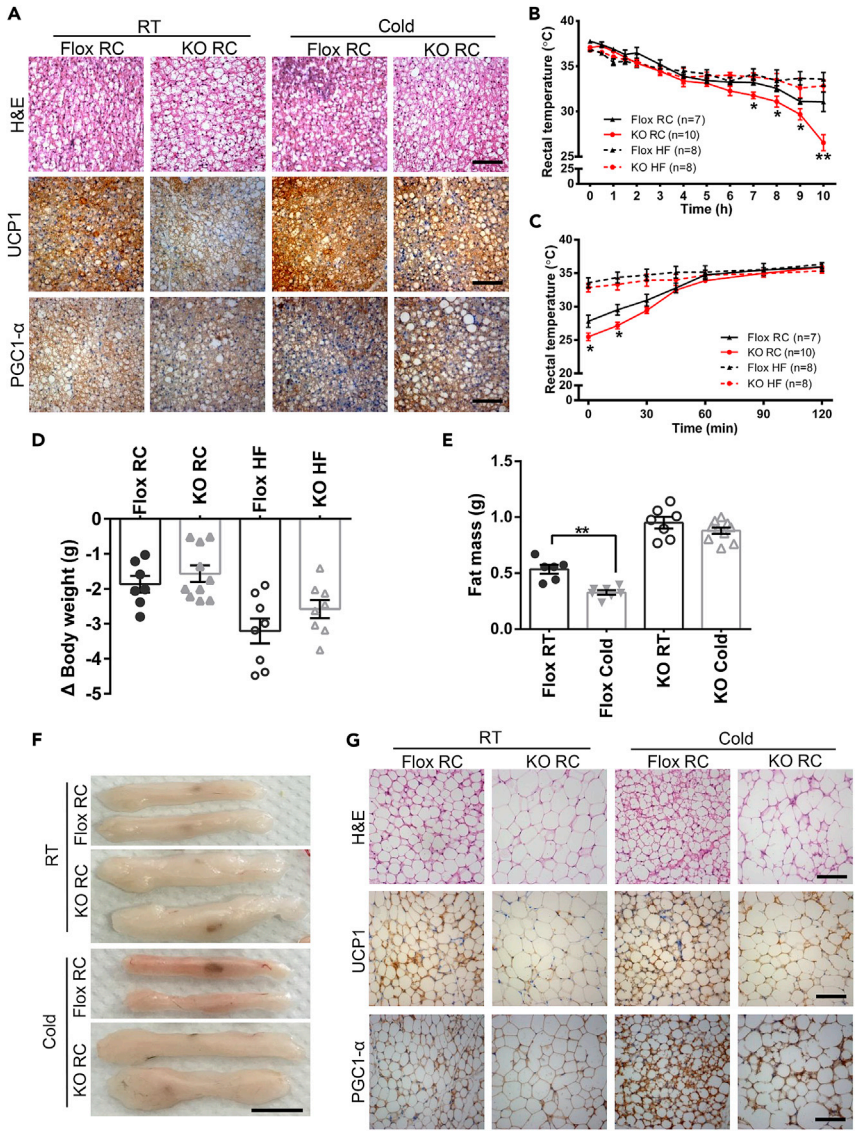

Figure 6. Ad-GHRKO Impairs Thermogenic Function and Significantly Inhibits Browning of SubQ WAT under Cold Stress

(A) H&E and Immunostaining of BAT from 16-week-old male Ad-GHRKO and Flox mice at room temperature or after 9-day cold stimulation. Scale bar, 100 μm.

(B) Body temperature of 16-week-old male Ad-GHRKO and Flox mice in the first day of cold stimulation.

(C) Body temperature recovery of 16-week-old male Ad-GHRKO and Flox mice at 25°C after first day of cold stimulation.

(D) Body weight reduction of 16-week-old Ad-GHRKO and Flox mice over 9-day cold stimulation.

(E) SubQ WAT mass of 16-week-old Ad-GHRKO and Flox mice over 9-day cold stimulation.

(F) Representative images of subQ WAT from 16-week-old male Ad-GHRKO and Flox mice at room temperature or after 9-day cold stimulation. Scale bar, 1 cm.

(G) H&E and Immunostaining of subQ WAT from 16-week-old male Ad-GHRKO and Flox mice at room temperature or after 9-day cold stimulation. Scale bar, 100 μm.

All values are presented as mean ± SEM. Statistical significance is shown as *$p \leq 0.05$ and **$p \leq 0.01$. See also Figures S2–S4.

DISCUSSION

GH is dubbed as an anti-obesity hormone for its actions of promoting lipolysis and inhibiting lipogenesis (Vijayakumar et al., 2010). Apart from the $GHR^{-/-}$ mice with global *Ghr* deletion and the FaGHRKO model, almost simultaneously and identical to our own design, an AdGHRKO model was generated by

List et al. (List et al., 2013, 2019). These models not only represent a longitudinal technique updating but also have made valuable attempts to describe the pleiotropic role of adipose GH/GHR from different perspectives. Taking the great chance to compare the phenotypes of these four mouse lines (Table S2), we found that the basal metabolic parameters of our Ad-GHRKO mice were overly parallel to List et al.'s AdGHRKO mice. Metabolic alterations in adipose tissues and at the systemic level in both male and female AdGHRKO mice were reported, whereas sexual dimorphism was avoided in the present study by examining only male subjects. Also, we particularly focused on the response of Ad-GHRKO mice to the metabolic stress of HF feeding and cold acclimation, which was not studied in both FaGHRKO and AdGHRKO mice.

In agreement with the AdGHRKO and in contrast to the $GHR^{-/-}$ mice, the endocrine production of GH and IGF-1 were not intervened by adipose *Ghr* deletion in our Ad-GHRKO mice, and the serum glucose levels were not affected under RC feeding. In clinical and mouse model studies, GH-deficient individuals are more likely to develop insulin resistance and fatty liver (Xu et al., 2012; Berryman et al., 2010). A concurrence of excessive WAT fat deposition and reduction of liver weight was described in both AdGHRKO (List et al., 2019) and our Ad-GHRKO mice, which counteract each other to retain a balanced body weight. Lowered liver weight was mainly attributed to the reduction of TG content. The most striking characteristic of Ad-GHRKO mice was that this hepatic protection was dramatically accentuated by HF feeding. Loss of adipose *Ghr* exacerbated subcutaneous obesity but inhibited ectopic adiposity in the liver and muscle tissues, another preferred site of pathological fat deposition (Figure S5). The serum lipid index and liver function markers, such as AST and ALT, were correspondingly less affected by dietary overloading in mice lacking adipose *Ghr*. In the study of AdGHRKO mice, the causes of the inhibition of liver steatosis were postulated as declined serum insulin concentration and improved insulin sensitivity. However, differing from the AdGHRKO mice, the baseline insulin level was unchanged in our Ad-GHRKO model and the enhanced insulin sensitivity was only observed after the mice were subjected to HF. This implies that the insulin response may protect the liver from adverse environmental cues, but other mechanisms must be also operating.

The adipocyte-produced, insulin-sensitizing hormone adiponectin is inversely associated with many metabolic disorders. Circulating levels of adiponectin were elevated in $GHR^{-/-}$ mice (List et al., 2011; Lubbers et al., 2013) but decreased in the FaGHRKO and the AdGHRKO mice (List et al., 2013, 2019). However, the regulation of adiponectin to improve insulin sensitivity may be overridden by the divergent adipokine profile displayed in the AdGHRKO mice, as no impact of systemic glucose tolerance and insulin sensitivity was found. Interestingly, in our Ad-GHRKO mice, although adiponectin secretion was stable under RC (Figure 1H), it was more profoundly stimulated by HF diet in the Ad-GHRKO mice than in the control mice (Flox 5,758.4 $\pm$ 125.2 ng/mL versus KO 6,622.9 $\pm$ 703.6 ng/mL). The amplified expansion of adipocyte size (hypertrophy) and number (hyperplasia) might lead to elevated adiponectin secretion, which correlated with improved insulin sensitivity.

By analyzing the lipogenic and lipolytic factors at both genetic and protein levels, and the adipocyte differentiation of SVF cells *in vitro*, we found that GH/GHR acted as the master regulator of the comprehensive lipid-producing machinery. The absence of adipose *Ghr* overwhelmingly based WAT-dominant obesity in Ad-GHRKO mice. Losing GHR control, the privileged local fat production in adipose, especially in subQ WAT, limited FFA availability to the liver and muscle by depleting substrate supply. The significant decline of β-HBA synthesis further verified the lower level of FFA disposal in the liver of Ad-GHRKO mice. Suppressed FFA releasing into the circulation, accompanied by accelerated TG clearance and FFA uptake in adipose, is a phenomenon documented in some forms of obesity (Kalant et al., 2000). On the other hand, an impaired peripheral FFA trapping was supposed to be the etiology of insulin resistance, dyslipidemia, and liver diseases secondary to HIV lipodystrophy (van Wijk et al., 2005). We propose a mechanism of FFA trapping in adipose tissue to prevent ectopic adiposity as a good trade-off of excessive fat hoarding in adipose, where *Ghr* plays an instrumental part (Figure 7).

The communication between adipose and liver, in respect of lipid metabolism and glucose homeostasis, has been investigated with different genetic engineering animal models. Some adipose-specific deletions of downstream post-receptor effectors of GH such as STAT5 in mice were studied and discussed (Johanna et al., 2011), but thus far the AdGHRKO and our Ad-GHRKO are the only mouse lines that underscored a clear-cut role of adipose GHR in fat draining from the liver to the adipose. The interorgan

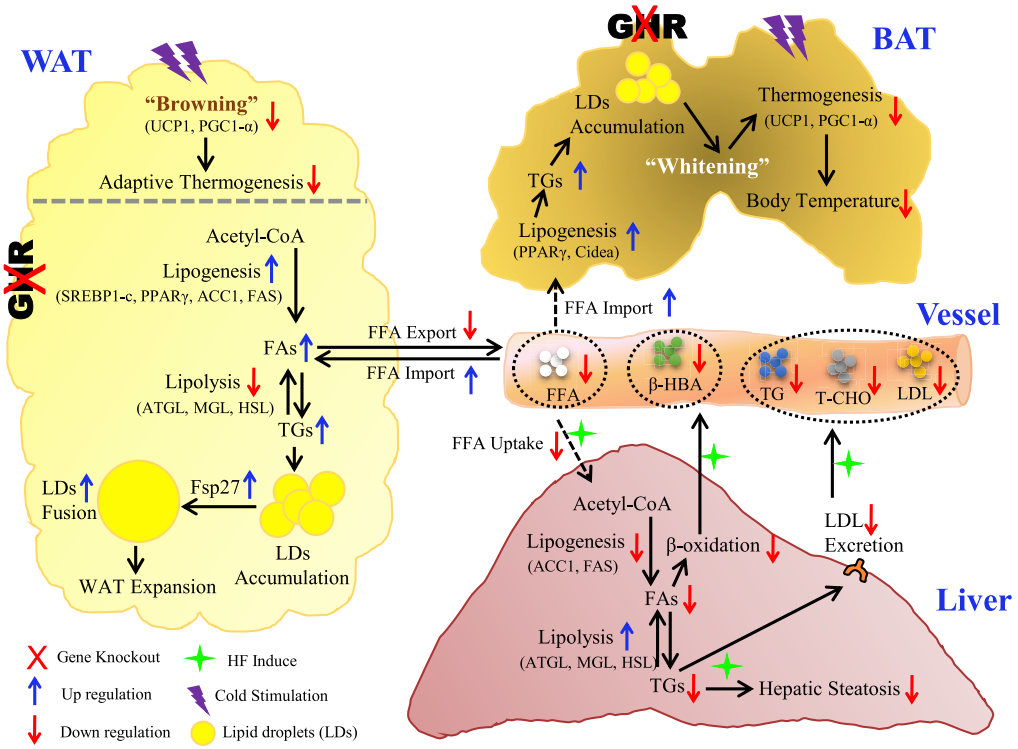

Figure 7. Schematic Summary of the Local and Systemic Impacts of Adipose *Ghr* Deletion, in Response to Metabolic Stress

Disruption of *Ghr* in adipose tissue significantly increases *de novo* lipogenesis and facilitates the lipid droplet fusion in both WAT and BAT. Excessive local adiposity resulting from HF diet constitutes an adipose FFAs trapping effect that spares dietary liver damage via limited FFA availability and liver FFA uptake. Meanwhile, lacking adipose *Ghr* causes a less effective adaptive thermogenic response to acute cold stimulation, whereas the body temperature under chronic cold stress can be stabilized by thermal insulation from subcutaneous fat compensation.

metabolic communication was also studied using genetically engineered animals lacking the key enzymes catalyzing lipolysis. The adipose-specific deletion of *Hsl*, rather than liver-specific *Hsl* deficiency, led to age-dependent lipodystrophy and liver steatosis (Xia et al., 2017), whereas intriguingly adipose-specific *Atgl*-KO mice had an opposite effect of reducing liver steatosis and improving hepatic insulin signaling (Schoiswohl et al., 2015). A similar liver protection from HF stress was reported in a systemic *Mgl*-KO mouse model, accompanied by appetite suppressing and decreased intestinal fat absorption (Yoshida et al., 2018).

The adaptive non-shivering thermogenesis mediated by UCP1-dependent activity in BAT is one of the facultative heat-producing strategies taken by mammals, especially in small animals, including rodents and infant humans, in response to limited nutrition supply or cold environment. Unlike the Ames dwarf mice and GHRKO mice, our Ad-GHRKO mice were less successful in maintaining normothermia, with declined gene expression and protein level of UCP1 and its regulator *Pgc1α*. WAT can acquire energy-burning potential by a "browning" process during which the white fat is converted into "beige." Stimulations activation of WAT browning includes endogenous hormonal regulation and exogenous stress, typically cold. The extra energy expenditure raised from WAT browning is recently proposed to be anti-obesity (Cohen and Spiegelman, 2015; Giralt and Villarroya, 2013). Consistent with recent data indicating that GH is able to promote WAT browning through activation of STAT5 (Nelson et al., 2018), we found that *Ghr* ablation in adipose tissues was able to inhibit browning of subQ WAT under cold stimulation. In Ad-GHRKO mice, the contained heat dissipation by BAT and the inhibited WAT browning conspired to safe-guard the fat storage attained from intensive energy intake. During the lipolysis processes, TGs from WAT are hydrolyzed into glycerol and FFAs. These FFAs then enter the mitochondria for lipid oxidation aimed to heat production. The low expression levels of lipolysis genes in WAT of Ad-GHRKO mice led to the

decrease of circulating FFAs, which could restrict the calorie sources of KO mice. Vice versa, the redundant subQ white fat formed an insulation layer to assist Ad-GHRKO mice against cold, which might justify the transient impairment of temperature maintenance in Ad-GHRKO mice.

In summary, aided by the Ad-GHRKO mouse model, we were able to test the distinct roles of adipose GHR in response to metabolic stress represented by HF feeding and cold acclimation. Defective adipose *Ghr* action endowed the mice with healthy fat storage in WAT: trapping fat within adipose tissues spared the liver from steatosis. However, "healthy" obesity was developed at the expense of impaired cold endurance and WAT browning (Figure 7). For populations feeding on a diet densely packed with calories, the double dictation of adipose GHR in both the metabolic dysfunctions centered at liver damage and the therapeutic or cosmetic weight management is of far-reaching interest. More mechanistic investigation of adipokines and cross-organ FFA messaging in the setting of GHR manipulation, in particular, generation of a liver- and adipose-specific double GHRKO mouse model is our immediate endeavor.

Limitations of the Study

The most significant evidence provided by this study is that adipose deletion of *Ghr* inhibited ectopic adiposity, especially in the liver, with a trade-off of subcutaneous fat expansion. However, there are several limitations owing to constraints on methodology and the scope of the research. (1) The inherent problem of the flox/Cre mouse model we used for adipose-specific *Ghr* knockout is that it did not provide platforms to discern the regulations of GH in metabolism from organ development, which could be achieved by temporally controlled *Ghr* knockout in mature or young growing animals using, e.g., tamoxifen-inducible technique. (2) Despite high specificity, Cre recombination efficiency in our Cre mouse line was not ideal, which might arise from the less-sensitive floxed allele and the critical roles GHR plays in adipogenesis and potentially cell survival of adipocytes themselves. (3) Experiments could have been performed to tease apart the different contributions of GHR in subcutaneous (SAT) versus visceral fat (VAT) to liver metabolism, such as fat tissue from a certain depot in Ad-GHRKO mouse could be transplanted into control mouse and the results would tell us if GHR signalings in SAT and VAT cooperate or counteract each other in metabolic regulations.

METHODS

All methods can be found in the accompanying Transparent Methods supplemental file.

SUPPLEMENTAL INFORMATION

Supplemental Information can be found online at https://doi.org/10.1016/j.isci.2019.05.020.

ACKNOWLEDGMENTS

This work was supported by the National Natural Science Foundation of China (No. 81600668; No. 81471000l); the Ministry of Science and Technology of China (No. 2014DFA32120); and Research Project of Educational Commission of Liaoning, China (No.L2016023).

AUTHOR CONTRIBUTIONS

Y.W. and L.R. conceived the study, designed the experiments, and wrote the manuscript. L.R. and X.W. performed experiments and collected and analyzed data. A.M., Y.L., and H.W. performed cold and cell experiments. J.W., J.S., and B.L. assisted with the qPCR and western Blot. M.G., D.W., W.G., and Y.L. performed animal breeding. R.J. and N.W. assisted with histological experiments. L.Z., L.H., X.C., B.L., and X.L. also designed the experiments and involved in discussion and writing the manuscript. L.Z., D.L., and X.L. provided language help. All authors reviewed the manuscript.

DECLARATION OF INTERESTS

The authors declare no competing interests.

Received: January 28, 2019
Revised: April 10, 2019
Accepted: May 13, 2019
Published: June 28, 2019

REFERENCES

Archana, V., Shoshana, Y., and Derek, L.R. (2011). The intricate role of growth hormone in metabolism. Front. Endocrinol. *2*, 1–11.

Arum, O., Boparai, R.K., Saleh, J.K., Wang, F., Dirks, A.L., Turner, J.G., Kopchick, J.J., Liu, J.L., Khardori, R.K., and Bartke, A. (2014). Specific suppression of insulin sensitivity in growth hormone receptor gene-disrupted (GHR-KO) mice attenuates phenotypic features of slow aging. Aging Cell *13*, 981–1000.

Baumann, G.P. (2009). Growth hormone isoforms. Growth Horm. IGF Res. *19*, 333–340.

Berryman, D.E., List, E.O., Kohn, D.T., Coschigano, K.T., Seeley, R.J., and Kopchick, J.J. (2006). Effect of growth hormone on susceptibility to diet-induced obesity. Endocrinology *147*, 2801–2808.

Berryman, D.E., List, E.O., Palmer, A.J., Chung, M.Y., Wright-Piekarski, J., Lubbers, E., O'connor, P., Okada, S., and Kopchick, J.J. (2010). Two-year body composition analyses of long-lived GHR null mice. J. Gerontol. A Biol. Sci. Med. Sci. *65*, 31–40.

Berryman, D.E., Glad, C.A., List, E.O., and Johannsson, G. (2013). The GH/IGF-1 axis in obesity: pathophysiology and therapeutic considerations. Nat. Rev. Endocrinol. *9*, 346–356.

Bond, L.M., and Ntambi, J.M. (2018). UCP1 deficiency increases adipose tissue monounsaturated fatty acid synthesis and trafficking to the liver. J. Lipid Res. *59*, 224–236.

Bonet, M.L., Mercader, J., and Palou, P. (2017). A nutritional perspective on UCP1-dependent thermogenesis. Biochimie *134*, 99–117.

Chathoth, S., Ismail, M.H., Vatte, C., Cyrus, C., Al Ali, Z., Ahmed, K.A., Acharya, S., Al Barqi, A.M., and Al Ali, A. (2018). Association of Uncoupling Protein 1 (UCP1) gene polymorphism with obesity: a case-control study. BMC Med. Genet. *19*, 203.

Cohen, P., and Spiegelman, B.M. (2015). Brown and beige fat: molecular parts of a thermogenic machine. Diabetes *64*, 2346–2351.

Coschigano, K.T., Clemmons, D., Bellush, L.L., and Kopchick, J.J. (2000). Assessment of growth parameters and life span of GHR/BP gene-disrupted mice. Endocrinology *141*, 2608–2613.

Coschigano, K.T., Holland, A.N., Riders, M.E., List, E.O., Flyvbjerg, A., and Kopchick, J.J. (2003). Deletion, but not antagonism, of the mouse growth hormone receptor results in severely decreased body weights, insulin, and insulin-like growth factor I levels and increased life span. Endocrinology *144*, 3799–3810.

Darcy, J., and Bartke, A. (2017). Functionally enhanced brown adipose tissue in Ames dwarf mice. Adipocyte *6*, 62–67.

Darcy, J., Mcfadden, S., Fang, Y., Huber, J.A., Zhang, C., Sun, L.Y., and Bartke, A. (2016). Brown adipose tissue function is enhanced in long-lived, male ames dwarf mice. Endocrinology *157*, 4744–4753.

Dominici, F.P., Arostegui Diaz, G., Bartke, A., Kopchick, J.J., and Turyn, D. (2000). Compensatory alterations of insulin signal transduction in liver of growth hormone receptor knockout mice. J. Endocrinol. *166*, 579–590.

Dreval, A.V., Trigolosova, I.V., Misnikova, I.V., Kovalyova, Y.A., Tishenina, R.S., and Barsukov, I.A. (2014). Prevalence of diabetes mellitus in patients with acromegaly. Endocr. Connect. *3*, 93–98.

Dulloo, A.G., and Schutz, Y. (2015). Adaptive thermogenesis in resistance to obesity therapies: issues in quantifying thrifty energy expenditure phenotypes in humans. Curr. Obes. Rep. *4*, 230–240.

Fan, Y., Menon, R.K., Cohen, P., Hwang, D., Clemens, T., Digirolamo, D.J., Kopchick, J.J., Le Roith, D., Trucco, M., and Sperling, M.A. (2009). Liver-specific deletion of the growth hormone receptor reveals essential role of growth hormone signaling in hepatic lipid metabolism. J. Biol. Chem. *284*, 19937–19944.

Flores-Morales, A., Greenhalgh, C.J., Norstedt, G., and Rico-Bautista, E. (2006). Negative regulation of growth hormone receptor signaling. Mol. Endocrinol. *20*, 241–253.

Freedman, D.S., Khan, L.K., Mei, Z., Dietz, W.H., Srinivasan, S.R., and Berenson, G.S. (2002). Relation of childhood height to obesity among adults: the bogalusa heart study. Pediatrics *109*, e23.

Giralt, M., and Villarroya, F. (2013). White, brown, beige/brite: different adipose cells for different functions? Endocrinology *154*, 2992–3000.

Guevara-Aguirre, J., and Rosenbloom, A.L. (2015). Obesity, diabetes and cancer: insight into the relationship from a cohort with growth hormone receptor deficiency. Diabetologia *58*, 37–42.

Han, G.S., Wu, W.I., and Carman, G.M. (2006). The Saccharomyces cerevisiae Lipin homolog is a Mg2+-dependent phosphatidate phosphatase enzyme. J. Biol. Chem. *281*, 9210–9218.

Janecka, A., Kołodziej-Rzepa, M., and Biesaga, B. (2016). Clinical and molecular features of laron syndrome, a genetic disorder protecting from cancer. In Vivo *30*, 375–381.

Jara, A., Liu, X., Sim, D., Benner, C.M., Duran-Ortiz, S., Qian, Y., List, E.O., Berryman, D.E., Kim, J.K., and Kopchick, J.J. (2016). Cardiac-specific disruption of GH receptor alters glucose homeostasis while maintaining normal cardiac performance in adult male mice. Endocrinology *157*, 1929–1941.

Johanna, L.B., Caroline, N.N., Mayumi, I., Lauren, A.M., Linda, M.K., Timothy, R.M., Elizabeth, E.P., and Michael, J.W. (2011). GH-dependent STAT5 signaling plays an important role in hepatic lipid metabolism. Endocrinology *152*, 181–192.

Kalant, D., Ph Lis, S., Fielding, B.A., Frayn, K.N., Cianflone, K., and Sniderman, A.D. (2000). Increased postprandial fatty acid trapping in subcutaneous adipose tissue in obese women. J. Lipid Res. *41*, 1963–1968.

Kozak, L.P., and Anunciado-Koza, R. (2008). UCP1: its involvement and utility in obesity. Int. J. Obes. (Lond.) *32* (*Suppl 7*), S32–S38.

Laron, Z. (2015). Lessons from 50 years of study of laron syndrome. Endocr. Pract. *21*, 1395–1402.

Laron, Z., Pertzelan, A., and Mannheimer, S. (1966). Genetic pituitary dwarfism with high serum concentation of growth hormone–a new inborn error of metabolism? Isr. J. Med. Sci. *2*, 152–155.

Lee, K.Y., Russell, S.J., Ussar, S., Boucher, J., Vernochet, C., Mori, M.A., Smyth, G., Rourk, M., Cederquist, C., Rosen, E.D., et al. (2013). Lessons on conditional gene targeting in mouse adipose tissue. Diabetes *62*, 864–874.

List, E.O., Sackmann-Sala, L., Berryman, D.E., Funk, K., Kelder, B., Gosney, E.S., Okada, S., Ding, J., Cruz-Topete, D., and Kopchick, J.J. (2011). Endocrine parameters and phenotypes of the growth hormone receptor gene disrupted (GHR-/-) mouse. Endocr. Rev. *32*, 356–386.

List, E.O., Berryman, D.E., Funk, K., Gosney, E.S., Jara, A., Kelder, B., Wang, X., Kutz, L., Troike, K., Lozier, N., et al. (2013). The role of GH in adipose tissue: lessons from adipose-specific GH receptor gene-disrupted mice. Mol. Endocrinol. *27*, 524–535.

List, E.O., Berryman, D.E., Funk, K., Jara, A., Kelder, B., Wang, F., Stout, M.B., Zhi, X., Sun, L., White, T.A., et al. (2014). Liver-specific GH receptor gene-disrupted (LiGHRKO) mice have decreased endocrine IGF-I, increased local IGF-I, and altered body size, body composition, and adipokine profiles. Endocrinology *155*, 1793–1805.

List, E.O., Berryman, D.E., Ikeno, Y., Hubbard, G.B., Funk, K., Comisford, R., Young, J.A., Stout, M.B., Tchkonia, T., Masternak, M.M., et al. (2015). Removal of growth hormone receptor (GHR) in muscle of male mice replicates some of the health benefits seen in global GHR-/- mice. Aging *7*, 500–512.

List, E.O., Berryman, D.E., Buchman, M., Parker, C., Funk, K., Bell, S., Duran-Ortiz, S., Qian, Y., Young, J.A., Wilson, C., et al. (2019). Adipocyte-specific GH receptor null (AdGHRKO) mice have enhanced insulin sensitivity with reduced liver triglycerides. Endocrinology *160*, 68–80.

Liu, J.L., Coschigano, K.T., Robertson, K., Lipsett, M., Guo, Y., Kopchick, J.J., Kumar, U., and Liu, Y.L. (2004). Disruption of growth hormone receptor gene causes diminished pancreatic islet size and increased insulin sensitivity in mice. Am. J. Physiol. Endocrinol. Metab. *287*, E405–E413.

Lu, C., Kumar, P.A., Sun, J., Aggarwal, A., Fan, Y., Sperling, M.A., Lumeng, C.N., and Menon, R.K. (2013). Targeted deletion of growth hormone (GH) receptor in macrophage reveals novel osteopontin-mediated effects of GH on glucose homeostasis and insulin sensitivity in diet-induced obesity. J. Biol. Chem. *288*, 15725–15735.

Lubbers, E.R., List, E.O., Jara, A., Sackman-Sala, L., Cordoba-Chacon, J., Gahete, M.D., Kineman, R.D., Boparai, R., Bartke, A., Kopchick, J.J., and Berryman, D.E. (2013). Adiponectin in mice with

altered GH action: links to insulin sensitivity and longevity? J. Endocrinol. *216*, 363–374.

Mavalli, M.D., Digirolamo, D.J., Fan, Y., Riddle, R.C., Campbell, K.S., and Van Groen, T. (2010). Distinct growth hormone receptor signaling modes regulate skeletal muscle development and insulin sensitivity in mice. J. Clin. Invest. *120*, 4007–4020.

Moller, N., and Jorgensen, J.O. (2009). Effects of growth hormone on glucose, lipid, and protein metabolism in human subjects. Endocr. Rev. *30*, 152–177.

Nelson, C.N., List, E.O., Ieremia, M., Constantin, L., Chhabra, Y., Kopchick, J.J., and Waters, M.J. (2018). Growth hormone activated STAT5 is required for induction of beige fat in vivo. Growth Horm. IGF Res. *2018*, 40–51.

Nicholls, D.G., and Locke, R.M. (1984). Thermogenic mechanisms in brown fat. Physiol. Rev. *64*, 1–64.

Peterson, T.R., Sengupta, S.S., Harris, T.E., Carmack, A.E., Kang, S.A., Balderas, E., Guertin, D.A., Madden, K.L., Carpenter, A.E., Finck, B.N., and Sabatini, D.M. (2011). mTOR complex 1 regulates lipin 1 localization to control the SREBP pathway. Cell *146*, 408–420.

Puigserver, P., Wu, Z., Park, C.W., Graves, R., Wright, M., and Spiegelman, B.M. (1998). A cold-inducible coactivator of nuclear receptors linked to adaptive thermogenesis. Cell *92*, 829–839.

Qi, Y., Sun, L., and Yang, H. (2017). Lipid droplet growth and adipocyte development: mechanistically distinct processes connected by phospholipids. Biochim. Biophys. Acta *1862*, 1273–1283.

Riordan, N.H., Ichim, T.E., Min, W.P., Wang, H., Solano, F., Lara, F., Alfaro, M., Rodriguez, J.P., Harman, R.J., Patel, A.N., et al. (2009). Non-expanded adipose stromal vascular fraction cell therapy for multiple sclerosis. J. Transl. Med. *7*, 29.

Rosenbloom, A.L. (1999). Growth hormone insensitivity: physiologic and genetic basis, phenotype, and treatment. J. Pediatr. *135*, 280–289.

Rui, L. (2017). Brown and beige adipose tissues in health and disease. Compr. Physiol. *7*, 1281–1306.

Schipper, H.S., Prakken, B., Kalkhoven, E., and Boes, M. (2012). Adipose tissue-resident immune cells: key players in immunometabolism. Trends Endocrinol. Metab. *23*, 407–415.

Schoiswohl, G., Stefanovic-Racic, M., Menke, M.N., Wills, R.C., Surlow, B.A., Basantani, M.K., Sitnick, M.T., Cai, L., Yazbec, K.C.F., Stolz, D.B., et al. (2015). Impact of reduced atgl-mediated adipocyte lipolysis on obesity-associated insulin resistance and inflammation in male mice. Endocrinology *156*, 3610–3624.

Schrauwen, P., Van Marken Lichtenbelt, W.D., and Spiegelman, B.M. (2015). The future of brown adipose tissues in the treatment of type 2 diabetes. Diabetologia *58*, 1704–1707.

Sjogren, K., Liu, J.L., Blad, K., Skrtic, S., Vidal, O., Wallenius, V., Leroith, D., Tornell, J., Isaksson, O.G., Jansson, J.O., and Ohlsson, C. (1999). Liver-derived insulin-like growth factor I (IGF-I) is the principal source of IGF-I in blood but is not required for postnatal body growth in mice. Proc. Natl. Acad. Sci. U S A *96*, 7088–7092.

Stovitz, S.D., Hannan, P.J., Lytle, L.A., Demerath, E.W., Pereira, M.A., and Himes, J.H. (2010). Child height and the risk of young-adult obesity. Am. J. Prev. Med. *38*, 0–77.

Sun, L.Y., and Bartke, A. (2014). Tissue-specific GHR knockout mice: metabolic phenotypes. Front. Endocrinol. (Lausanne) *5*, 243.

Vijayakumar, A., Novosyadlyy, R., Wu, Y., Yakar, S., and Leroith, D. (2010). Biological effects of growth hormone on carbohydrate and lipid metabolism. Growth Horm. IGF Res. *20*, 1–7.

Vijayakumar, A., Wu, Y., Buffin, N.J., Li, X., Sun, H., Gordon, R.E., Yakar, S., and Leroith, D. (2012a). Skeletal muscle growth hormone receptor signaling regulates basal, but not fasting-induced, lipid oxidation. PLoS One *7*, e44777.

Vijayakumar, A., Wu, Y., Sun, H., Li, X., Jeddy, Z., Liu, C., Schwartz, G.J., Yakar, S., and Leroith, D. (2012b). Targeted loss of GHR signaling in mouse skeletal muscle protects against high-fat diet-induced metabolic deterioration. Diabetes *61*, 94–103.

Wang, Z.V., Deng, Y., Wang, Q.A., Sun, K., and Scherer, P.E. (2010). Identification and characterization of a promoter cassette conferring adipocyte-specific gene expression. Endocrinology *151*, 2933–2939.

van Wijk, J.P., Cabezas, M.C., De Koning, E.J., Rabelink, T.J., Van, D.G.R., and Hoepelman, I.M. (2005). In vivo evidence of impaired peripheral fatty acid trapping in patients with human immunodeficiency virus-associated lipodystrophy. J. Clin. Endocrinol. Metab. *90*, 3575–3582.

Wu, Y., Liu, C., Sun, H., Vijayakumar, A., Giglou, P.R., Qiao, R., Oppenheimer, J., Yakar, S., and Leroith, D. (2011). Growth hormone receptor regulates beta cell hyperplasia and glucose-stimulated insulin secretion in obese mice. J. Clin. Invest. *121*, 2422–2426.

Xia, B., Cai, G.H., Yang, H., Wang, S.P., Mitchell, G.A., and Wu, J.W. (2017). Adipose tissue deficiency of hormone-sensitive lipase causes fatty liver in mice. PLoS Genet. *13*, e1007110.

Xu, L., Xu, C., Yu, C., Miao, M., Zhang, X., Zhu, Z., Ding, X., and Li, Y. (2012). Association between serum growth hormone levels and nonalcoholic fatty liver disease: a cross-sectional study. PLoS One *7*, e44136.

Yoshida, K., Kita, Y., Tokuoka, S.M., Hamano, F., Yamazaki, M., Sakimura, K., Kano, M., and Shimizu, T. (2018). Monoacylglycerol lipase deficiency affects diet-induced obesity, fat absorption, and feeding behavior in CB1 cannabinoid receptor-deficient mice. FASEB J. *33*, 2484–2497.

Zhou, Y., Xu, B.C., Maheshwari, H.G., He, L., Reed, M., Lozykowski, M., Okada, S., Cataldo, L., Coschigamo, K., Wagner, T.E., et al. (1997). A mammalian model for Laron syndrome produced by targeted disruption of the mouse growth hormone receptor/binding protein gene (the Laron mouse). Proc. Natl. Acad. Sci. U S A *94*, 13215–13220.

ISCI, Volume *16*

Supplemental Information

Loss of Adipose Growth Hormone Receptor in Mice Enhances Local Fatty Acid Trapping and Impairs Brown Adipose Tissue Thermogenesis

Liyuan Ran, Xiaoshuang Wang, Ai Mi, Yanshuang Liu, Jin Wu, Haoan Wang, Meihua Guo, Jie Sun, Bo Liu, Youwei Li, Dan Wang, Rujiao Jiang, Ning Wang, Wenting Gao, Li Zeng, Lin Huang, Xiaoli Chen, Derek LeRoith, Bin Liang, Xin Li, and Yingjie Wu

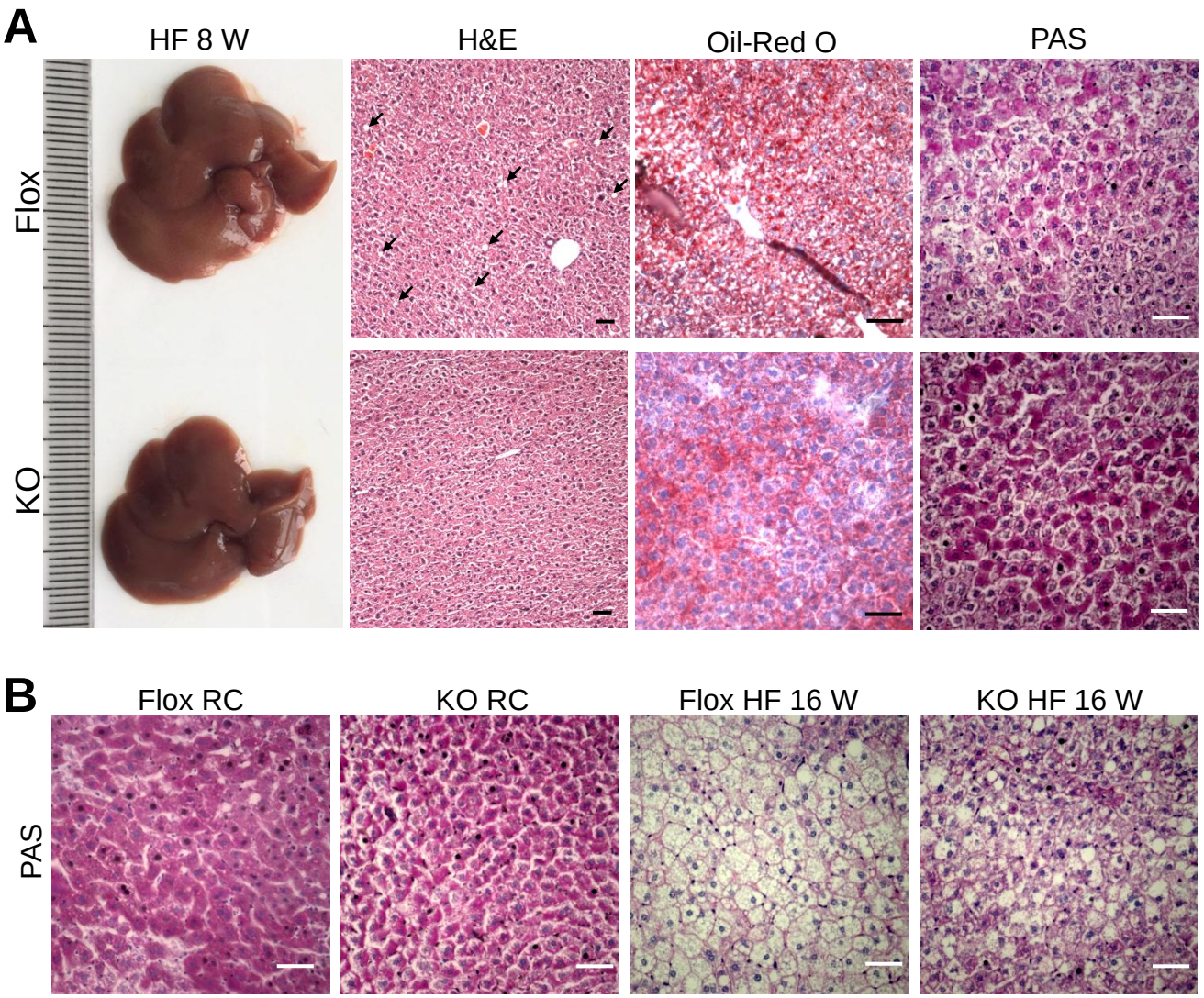

Figure S1: Ad-GHRKO Alleviates Hepatic Steatosis and Promotes Glycogen Synthesis during HF Feeding. Related to Figure 2 and 5.

(A) Representative images of liver from 16-week-old male Ad-GHRKO and Flox mice (HF fed for 8weeks), and H&E, Oil-Red O and PAS staining of liver sections. Scale bar, 50 μm.

(B) PAS staining of liver sections of 24-week-old male Ad-GHRKO and Flox mice (HF fed for 16 weeks). Scale bar, 50 μm.

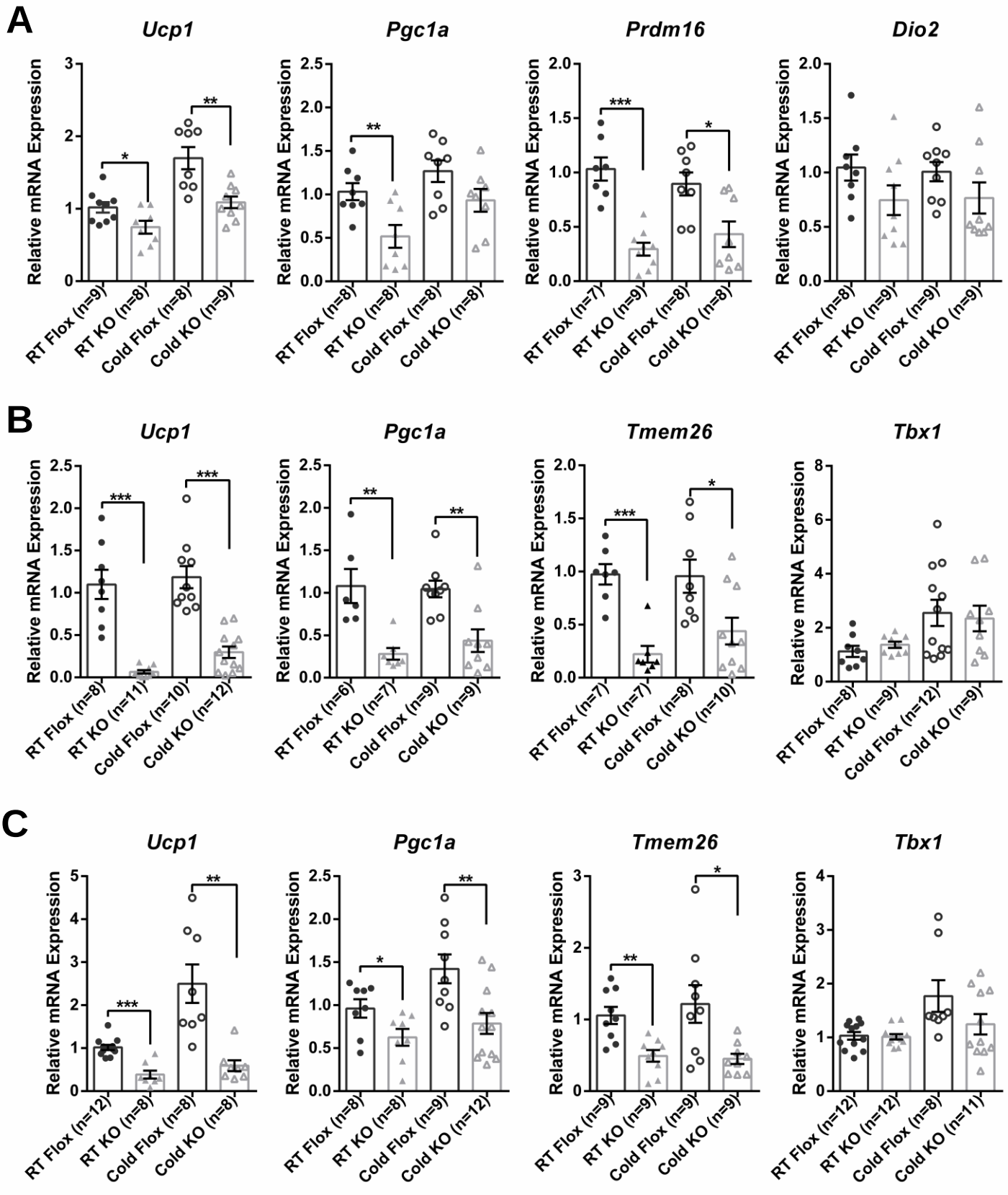

Figure S2: Relative mRNA Expression Levels of Genes in BAT (A), SubQ WAT (B) and Epi WAT (C) of 16-week-old male Ad-GHRKO and Flox mice (HF fed for 8 weeks). Data are represented as mean ± SEM. Related to Figure 6.

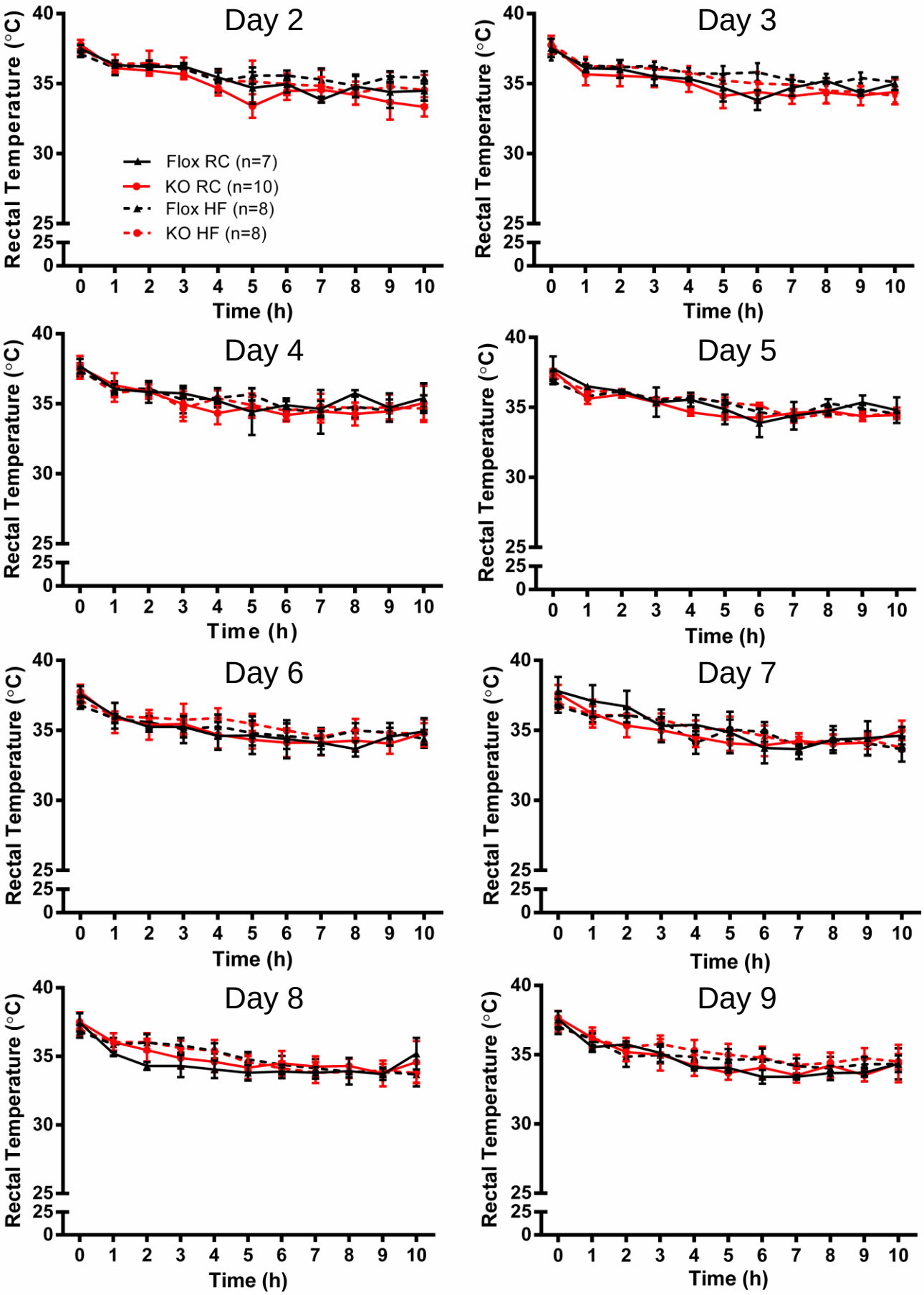

Figure S3: Body Temperature from Day 2 to Day 9 of Cold Stimulation. Data are represented as mean ± SEM. Related to Figure 6.

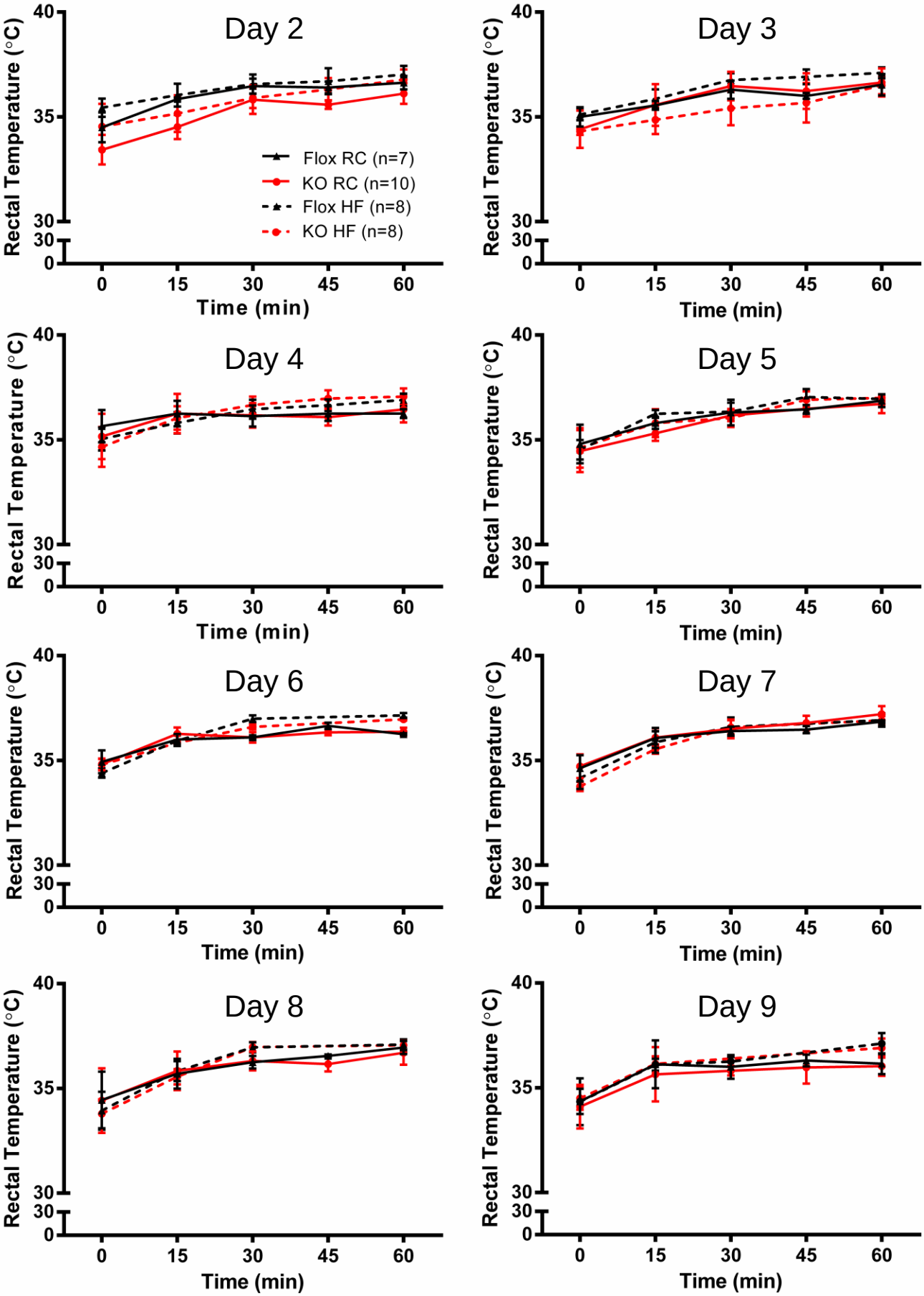

Figure S4: Body Temperature Recovery of the Mice at 25°C from Day 2 to Day 9 of Cold Stimulation. Data are represented as mean ± SEM. Related to Figure 6.

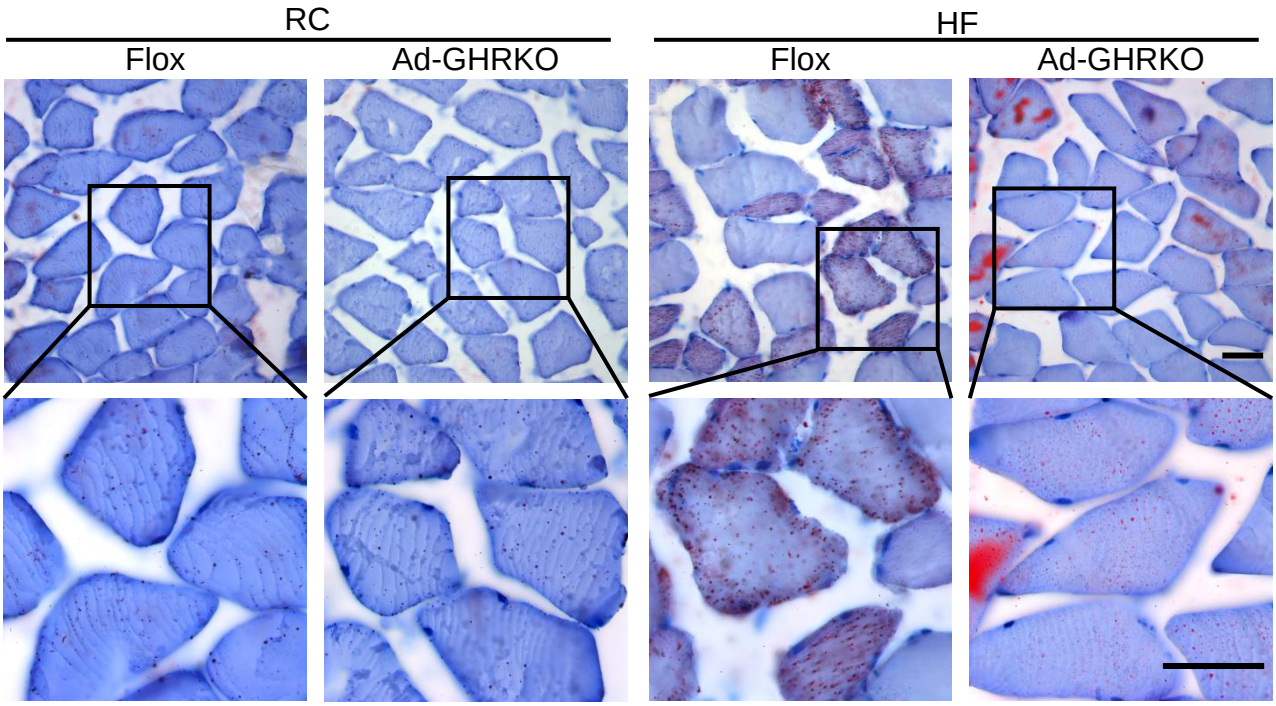

Figure S5: Lipid Accumulation Visualized by Oil-Red O Staining on Muscle Sections of 24-week-old Male Ad-GHRKO and Flox Mice. Related to Figure 2 and 5.
No obvious difference in muscles was found between RC groups. HF diet induced evidently more lipid accumulation in muscles of Flox mice than that of the KO mice. Scale bar, 50 μm.

Table S1. Primer sequences. Related to Figure 1, 3, 4, 5 and Figure S2.

Gene		primer
Ghr	Forward	5'-CATTCTTTTCTGGGATGCTAT-3'
	Reverse	5'-CGGACATTGCATCTGTGATT-3'
Adipo-Cre	Forward	5'-GGATGTGCCATGTGAGTCTG-3'
	Reverse	5'-ACGGACAGAAGCATTTTCCA-3'
Acc1	Forward	5'-TGCCACCACCTTATCACTATGTA-3'
	Reverse	5'-CCTGCCTGTCTCCATCCA-3'
Fas	Forward	5'-TCGTCTATACCACTGCTTACTAC-3'
	Reverse	5'-ACACCACCTGAACCTGAG-3'
Atgl	Forward	5'-GCTGTGGAATGAGGACATAGGA-3'
	Reverse	5'-GCATAGTGAGTGGCTGGTGAA-3'
Hsl	Forward	5'-TGTGTCAGTGCCTATTCAG-3'
	Reverse	5'-GAACAGCGAAGTGTCTCT-3'
Mgl	Forward	5'-GCTGTGGAATGAGGACATAGGA-3'
	Reverse	5'-GCATAGTGAGTGGCTGGTGAA-3'
Pparγ	Forward	5'-TGTGGACCTCTCCGTGATGG-3'
	Reverse	5'-GGTTCTACTTTGATCGCACTTTGG-3'
Fsp27	Forward	5'-TTGATGTGGCCCGTGTAACGTTTG-3'
	Reverse	5'-AAGCTTCCTTCATGATGCGCTTGG-3'
Prdm16	Forward	5'-TGAGGAAGCATTTGAAGTTAAAG-3'
	Reverse	5'-GTTCTTAGCCTGCCTGTAC-3'
Pgc1α	Forward	5'-CCGAAGACACTACAGGTTCCATAG-3'
	Reverse	5'-GGGAGGGAGAGAGGAGAGAGG-3'
Ucp1	Forward	5'-AAGACAGAAGAGCATAGCATTCAC-3'
	Reverse	5'-CCAGTCATACACTCCCACCTC-3'
Tbx1	Forward	5'-CACCGGATCACGCAGCTTAAG-3'
	Reverse	5'-GCAGCGTCTTTGTCTGAGCC-3'
Tmem26	Forward	5'-GTGGTGTGGACGTGGAGTATGC-3'
	Reverse	5'-GTAGATCATCAGGACGAGGCGC-3'
Cide a	Forward	5'-TGACATTCATGGGATTGCAGAC-3'
	Reverse	5'-GGCCAGTTGTGATGACTAAGAC-3'
Dio2	Forward	5'-AATTATGCCTCGGAGAAGACCG-3'
	Reverse	5'-GGCAGTTGCCTAGTGAAAGGT-3'
Srebp1	Forward	5'-CGGAGCCATGGATTGCACTTTC-3'
	Reverse	5'-GATGCTCAGTGGCACTGACTCTTC-3'
Ppara	Forward	5'-AGAGCCCCATCTGTCCTCTC-3'
	Reverse	5'-ACTGGTAGTCTGCAAAACCAAA-3'
Cpt1b	Forward	5'-AAGAGACCCCGTAGCCATCAT-3'
	Reverse	5'-GACCCAAAACAGTATCCCAATCA-3'
Cpt2	Forward	5'-CAAAAGACTCATCCGCTTTGTTC-3'
	Reverse	5'-CATCACGACTGGGTTTGGGTA-3'
Atp5a	Forward	5'-TCTCCATGCCTCTAACACTCG-3'

Fabp3	Reverse	5'-CCAGGTCAACAGACGTGTCAG-3'
	Forward	5'-ACCAAGCCTACTACCATCATCG-3'
	Reverse	5'-CCTCGTCGAACTCTATTCCCAG-3'
Cd36	Forward	5'-TTGAAAAGTCTCGGACATTGAG-3'
	Reverse	5'-TCAGATCCGAACACAGCGTA-3'
Fabp1	Forward	5'-GTCAGAAATCGTGCATGAAGGG-3'
	Reverse	5'-GAACTCATTGCGGACCACTTT-3'
Fatp2	Forward	5'-GATGCCGTGTCCGTCTTTTAC-3'
	Reverse	5'-GACTTCAGACCTCCACGACTC-3'
Fatp5	Forward	5'-GTTCTCCCGTCCAAGACCATT-3'
	Reverse	5'-GCTCCGTACAGAGTGTAGCAAG-3'
Gapdh	Forward	5'-GGGCTGGCATTGCTCTCAATG-3'
	Reverse	5'-CATGTAGGCCATGAGGTCCAC-3'

Table S2. Phenotype summary of *Ghr* knockout mouse lines. Related to Figure 1, 2, 3 and 5.

	GHRKO[a]	**FaGHRKO[b]**	**AdGHRKO[c]**	**Ad-GHRKO[d]**
Body Weight	↓	↑	≈	≈, HF↑
Body Length	↓	↑	≈	≈
GH	↑	≈	≈	≈
IGF-1	↓	↑	≈	≈
Insulin	↓	≈	↓	≈
Blood Glucose	≈↓	≈	≈	≈, HF↓
Glucose Tolerance	Impaired	≈	≈	≈, HF Enhanced
Insulin Sensitivity	Enhanced	≈	Enhanced	≈, HF Enhanced
Fat/BW %	↑	↑	↑	↑
SubQ WAT Mass	↑	↑	↑	↑
Adipocyte Size	↑	↑	↑	↑
Liver/BW %	↓	≈	↓	↓
Liver TG	↑	≈	↓	↓

Note: [a]GHRKO: *Ghr* gene total knockout mouse model (Berryman et al., 2010, Zhou et al., 1997, Berryman et al., 2006, Liu et al., 2004, Coschigano et al., 2003); [b]FaGHRKO: Fat-specific *Ghr* gene knockout mouse model driven by ap2 promoter (List et al., 2013); [c]AdGHRKO: Adipose-specific *Ghr* gene knockout mouse model driven by adiponectin promoter (List EO et al., 2018); [d]Ad-GHRKO: Adipose-specific *Ghr* gene knockout mouse modelin this study. BW: body weight; TG, triglyceride; ↑, increased; ↓, decreased; ≈, no significant changes; HF, high-fat diet.

Transparent Methods

Generation of Adipose Tissue-specific *Ghr* Knockout Mice

All animal experiments were performed under the guidelines for the treatment of laboratory animals and were approved by the Committee on the Ethics of Animal Experiments of Dalian Medical University. Heterozygous mice were generated by crossing *Ghr*-Floxed mice (Wu et al., 2011, Wu et al., 2009b) with mice expressing Cre recombinase under the control of the adiponectin promoter (B6; FVB-Tg (Adipoq-Cre)1Evdr/J, Jackson Laboratory, Stock No 010803). Adipose tissue-specific *Ghr* knockout mice (Ad-GHRKO) were created by crossing the heterozygous mice. The floxed littermates were used as control. Only the male Ad-GHRKO and control mice were examined in the subsequent experiments. Mouse genotyping was performed by PCR using primers shown in Table S1. Mice were fed with RC (D12450J, 10% kcal from fat, Research Diets, Inc., New Brunswick, NJ) or HF diet (D12492, 60% kcal from fat, Research Diets, Inc., New Brunswick, NJ) and maintained in a temperature- and humidity-controlled room on a 12-h light/dark cycle at Specific Pathogen Free Experimental Animal Center of Dalian Medical University.

Body Weight, Organ Weight and Serum Analysis

Body weights were measured every two weeks during the entire experimental period. Blood glucose concentrations were measured with glucometers (ACCU-CHEK). Glucose Tolerance Tests (GTT, 2.0 g glucose per kg of body weight) and Insulin Tolerance Tests (ITT, 0.75 unit of recombinant human insulin (Becton Dickinson and Company) per kg of body weight) were performed as described previously (Wu et al.,

2009a). Organ dissections were weighed on ananalytical balance and snap-frozen in liquid nitrogen before being stored at -80^{o}C. Serum was separated from the whole blood by centrifugation at 4000 rpm for 15 min at 4^{o}C and stored at -80^{o}C for further use. Serum triglyceride (TG) (A110-1), total cholesterol (T-CHO) (A111-1), high-density lipoprotein cholesterol (HDL-C) (A112-2), low-density lipoprotein cholesterol (LDL-C) (A113-2), non-esterified fatty acid (NEFA) (A042-2), aspartate aminotransferase (AST) (C010-1) and alanine aminotransferase (ALT) (C009-1) levels were measured using ELISA kits (Jian Cheng Biological Engineering Institute, Nanjing, China) according to the manufacturer's instructions. Serum GH (BPE20916), IGF-1 (BPE20004), insulin (BPE20353) and β-Hydroxybutyric acid (β-HBA) (BPE20760) were measured using ELISA kits (Lengton Bioscience Co.LTD, Shanghai, China), according to the manufacturer's instructions.

Gene Expression Assessment by Real Time PCR

Tissue samples were saved in RNAhold (EH101, TransGen). Total RNA was extracted from frozen tissues using RNAiso Plus kit (9109, Takara) following the manufacturer's protocol and then reverse transcribed using a primeScript™ RT reagent kit (RR047A, Takara). The levels of mRNA expression were quantified by real-time PCR using a TransStart Tip Green qPCR SuperMix kit (AQ142, TransGen). *Gapdh* was used as the endogenous control. The primers used for qPCR were listed in Supplementary Table S1.

Protein Extraction and Western Blot

Proteins were extracted from frozen tissues using RIPA lysis buffer (R0020, Solarbio) containing protease inhibitor cocktail (P1006, Beyotime). Protein concentrations were quantified by BCA Assay Kit (P0012, Beyotime). Equal amount of proteins was separated with SDS-PAGE, and then transferred to nitrocellular membrane for probing with the indicated antibodies. The following primary antibodies were used: GAPDH (10494-1-AP, Proteintech), Tubulin (Abp52656, Abbkine), ACC1 (4190S, CST), FAS (60196-1-IG, Proteintech), PPARα (15540-1-AP, Proteintech), Lipin1 (GTX115676, GeneTex), PPARγ (16643-1-AP, Proteintech), ATGL (bs-3831R, Bioss), CD36 (18836-1-AP, Proteintech) and SREBP1 (14088-1-AP, Proteintech). Anti-rabbit secondary antibody and ECL detection reagent were purchased from Proteintech.

H&E, IHC, Oil Red-O and PAS Staining

Fat and liver tissues were fixed with 10% formalin for at least 24 hrs. For H&E staining, tissues were embedded in paraffin and sectioned into 8 μm intervals (Leica), and then stained with H&E. For immunohistochemistry (IHC), tissue sections were deparaffinized, rehydrated and permeated using Triton X 100 (0694, Amresco), and followed by antigen retrieval using heat-induced citrate solution (C1032, Solarbio). IHC staining was performed using SP link Detection kit (SP-9001, Zsgb-Bio) and DAB kit (ZLI-9017, Zsgb-Bio) according to the instructions. Antibodies used: anti-UCP1 (GTX112784, GeneTex) and anti-PGC1α (bs-7535R, Bioss). For lipid staining, liver tissues were cut into 10 μm sections at -20^{o}C and sucrose dehydrated, followed by staining with Oil Red-O (D027, Njjcbio). The glycogen accumulation in

the liver was detected by staining the dewaxed liver tissue sections with periodic acid-schiff (PAS, G1281, Solarbio) according to the manufacturer's instructions. The slides were observed using Nikon Ni-E microscope to collect images. The average area of adipocyte cells was analyzed using Image J software on H&E slides from at least three 200× fields of three mice per genotype.

Liver TG Assay

Equal weights of frozen liver tissues were homogenized in ethanol. Samples were centrifuged at 12000 rpm for 10 min and supernatants were collected for TG determination with TG Assay kit (A110-1, Jian Cheng Biological Engineering Institute, Nanjing, China).

SVF Cell Differentiation

Primary stromal vascular fraction (SVF) cells from WAT and BAT of 20-week-old Ad-GHRKO or Flox mice were isolated with the method described previously (Ghorbani and Abedinzade, 2013). The collected SVF cells were seeded at a density of 5,000 cells per cm^2 in DMEM (SH30081.01, Hyclone) with 10% fetal bovine serum (Catalog 100-500, GemCell™), 1× Penicillin-Streptomycin solution (P1400, Solarbio) and 2.5 μg/ml Amphotericin B (CA2021, Coolaber) and cultured for two passages. The cells were then reseeded at a density of 40,000 cells per well in 12-well plates. Differentiation of SVF cells was achieved by culturing the cells in the adipogenic induction medium (MUBMD-90031, Cyagen) for 9 days in a humidified incubator at 37^oC with 5% CO_2. Palmitic acid (PA, H8780, Solarbio) was used to

simulate the HF environment. Once mature adipocytes formation was determined, the cells were fixed with 10 % formalin and stained with Oil Red-O.

Cold Exposure Experiment

The 16-week-old male Ad-GHRKO and Flox mouse groups were each randomly divided into two parallel subgroups. While one sub-group remained at room temperature, the matched subgroup was exposed to 4^{o}C on a 10-h/14-h cycle for 9 days. Mice in all groups were individually housed in a clean cage, with free access to water but no food during the cold episode. The rectal temperature of the mice was measured at various times from the start of cold exposure until back to room temperature for 2 hrs.

Statistical Analyses

All data are shown as mean ± SEMs. Statistical analysis was performed by a Student's t test using GraphPad Prism software. Statistical significance was indicated by *P≤0.05, **P≤0.01 and ***P≤0.001.

References

BERRYMAN, D. E., LIST, E. O., KOHN, D. T., COSCHIGANO, K. T., SEELEY, R. J. & KOPCHICK, J. J. 2006. Effect of growth hormone on susceptibility to diet-induced obesity. *Endocrinology,* 147**,** 2801-8.

BERRYMAN, D. E., LIST, E. O., PALMER, A. J., CHUNG, M. Y., WRIGHT-PIEKARSKI, J., LUBBERS, E., O'CONNOR, P., OKADA, S. & KOPCHICK, J. J. 2010. Two-year body composition analyses of long-lived GHR null mice. *J Gerontol A Biol Sci Med Sci,* 65**,** 31-40.

COSCHIGANO, K. T., HOLLAND, A. N., RIDERS, M. E., LIST, E. O., FLYVBJERG, A. & KOPCHICK, J. J. 2003. Deletion, but not antagonism, of the mouse growth hormone receptor results in severely decreased body weights, insulin, and insulin-like growth factor I levels and increased life span. *Endocrinology,* 144**,** 3799-810.

GHORBANI, A. & ABEDINZADE, M. 2013. Comparison of in vitro and in situ methods for studying lipolysis. *ISRN Endocrinol,* 2013**,** 205385-205390.

LIST EO, BERRYMAN DE, BUCHMAN M, PARKER C, FUNK K, BELL S,

DURAN-ORTIZ S, QIAN Y, YOUNG JA, WILSON C, SLYBY J, MCKENNA S, JENSEN EA & JJ., K. 2018. Adipocyte-specific GH receptor null (AdGHRKO) mice have enhanced insulin sensitivity with reduced liver triglycerides. *Endocrinology.***,** Epub ahead of print.

LIST, E. O., BERRYMAN, D. E., FUNK, K., GOSNEY, E. S., JARA, A., KELDER, B., WANG, X., KUTZ, L., TROIKE, K., LOZIER, N., MIKULA, V., LUBBERS, E. R., ZHANG, H., VESEL, C., JUNNILA, R. K., FRANK, S. J., MASTERNAK, M. M., BARTKE, A. & KOPCHICK, J. J. 2013. The role of GH in adipose tissue: lessons from adipose-specific GH receptor gene-disrupted mice. *Mol Endocrinol,* 27**,** 524-35.

LIU, J. L., COSCHIGANO, K. T., ROBERTSON, K., LIPSETT, M., GUO, Y., KOPCHICK, J. J., KUMAR, U. & LIU, Y. L. 2004. Disruption of growth hormone receptor gene causes diminished pancreatic islet size and increased insulin sensitivity in mice. *Am J Physiol Endocrinol Metab,* 287**,** E405-13.

WU, Y., LIU, C., SUN, H., VIJAYAKUMAR, A., GIGLOU, P. R., QIAO, R., OPPENHEIMER, J., YAKAR, S. & LEROITH, D. 2011. Growth hormone receptor regulates beta cell hyperplasia and glucose-stimulated insulin secretion in obese mice. *J Clin Invest,* 121**,** 2422-6.

WU, Y., SUN, H., YAKAR, S. & LEROITH, D. 2009a. Elevated levels of insulin-like growth factor (IGF)-I in serum rescue the severe growth retardation of IGF-I null mice. *Endocrinology,* 150**,** 4395-403.

WU, Y., WANG, C., SUN, H., LEROITH, D. & YAKAR, S. 2009b. High-efficient FLPo deleter mice in C57BL/6J background. *PLoS One,* 4**,** e8054.

ZHOU, Y., XU, B. C., MAHESHWARI, H. G., HE, L., REED, M., LOZYKOWSKI, M., OKADA, S., CATALDO, L., COSCHIGAMO, K., WAGNER, T. E., BAUMANN, G. & KOPCHICK, J. J. 1997. A mammalian model for Laron syndrome produced by targeted disruption of the mouse growth hormone receptor/binding protein gene (the Laron mouse). *Proc Natl Acad Sci U S A,* 94**,** 13215-20.